Sources of Ionizing Radiation and Radiation Interactions

Reading Material:

Chapter 1, Radiation Detection and Measurements,

Forth Edition, by G. F. Knoll

Table of Contents

I. Radiation Sources
- Sources of Fast Electron and Heavy Charged Particles
- Gamma Rays Sources
- X-Rays Sources
- Neutron Sources

II. Radiation Interactions
- Interactions of X ray and Gamma Rays
- Interactions of Fast Electrons and Heavy Charged Particles.
- Interactions of Neutrons

Common isotopes used in nuclear medicine [9][10]

isotope	symbol	Z	$T_{1/2}$	decay	gamma (keV)	positron (keV)
Imaging:						
fluorine-18	^{18}F	9	109.77 m	β^+	511 (193%)	249.8 (97%)[11]
gallium-67	^{67}Ga	31	3.26 d	ec	93 (39%), 185 (21%), 300 (17%)	-
krypton-81m	^{81m}Kr	36	13.1 s	IT	190 (68%)	-
rubidium-82	^{82}Rb	37	1.27 m	β^+	511 (191%)	3.379 (95%)
nitrogen-13	^{13}N	7	9.97 m	β^+	511 (200%)	1190 (100%)[12]
technetium-99m	^{99m}Tc	43	6.01 h	IT	140 (89%)	-
indium-111	^{111}In	49	2.80 d	ec	171 (90%), 245 (94%)	-
iodine-123	^{123}I	53	13.3 h	ec	159 (83%)	-
xenon-133	^{133}Xe	54	5.24 d	β^-	81 (31%)	0.364 (99%)
thallium-201	^{201}Tl	81	3.04 d	ec	69–83* (94%), 167 (10%)	-
Therapy:						
yttrium-90	^{90}Y	39	2.67 d	β^-	-	2.280 (100%)
iodine-131	^{131}I	53	8.02 d	β^-	364 (81%)	0.807 (100%)

Z = atomic number, the number of protons; $T_{1/2}$ = half-life; decay = mode of decay

photons = principle photon energies in kilo-electron volts, keV, (abundance/decay)

β = beta maximum energy in mega-electron volts, MeV, (abundance/decay)

$\beta^+ = \beta^+$ decay; $\beta^- = \beta^-$ decay; IT = isomeric transition; ec = electron capture

* X-rays from progeny, mercury, Hg

Beta Decay

Things to consider from imaging view point

- Types of particles emitted, gamma ray, X-ray, fast electrons, Auger electrons, and their corresponding
- half-life,
- energy, and
- relative intensity.

Beta Emission

- Beta particle is an ordinary electron. Many atomic and nuclear processes result in the emission of beta particles.
- One of the most common source of beta particles is the beta decay of nuclides, in which

Beta decay

$$ {}^{A}_{Z}X \rightarrow {}^{A}_{Z+1}Y + {}^{0}_{-1}\beta + \bar{\upsilon} $$

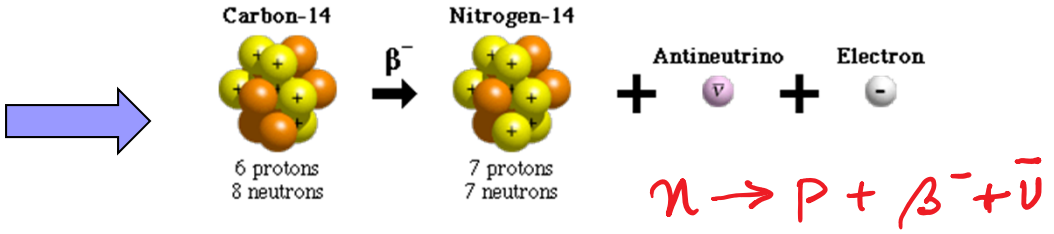

Beta-plus decay

$$ {}^{A}_{Z}X \rightarrow {}^{A}_{Z-1}Y + {}^{0}_{1}\beta + \upsilon $$

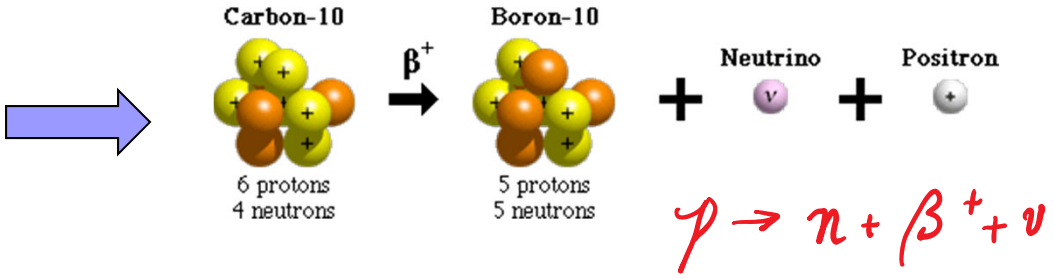

Electron capture

$$ {}^{A}_{Z}X + e^{-} \rightarrow {}^{A}_{Z-1}Y + \upsilon $$

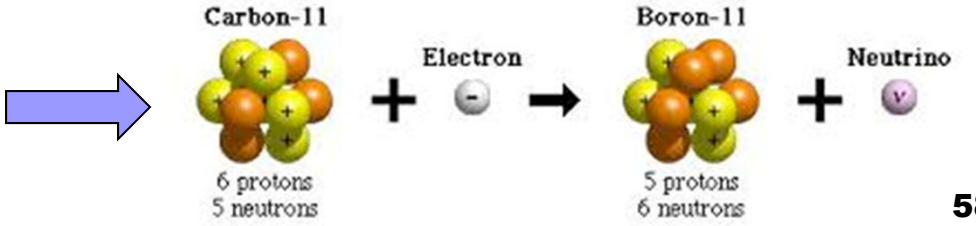

“Regular” Beta Decay

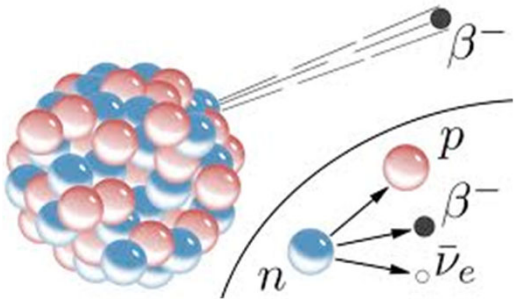

Energy Release of Beta Decay

The energy release in a beta decay is given as

$$Q = M_p - (M_d + M_e)$$

- The energy release is once again given by the conversion of a fraction of the mass into energy. Note that atomic electron bonding energy is neglected.
- For a beta decay to be possible, the energy release has to be positive.

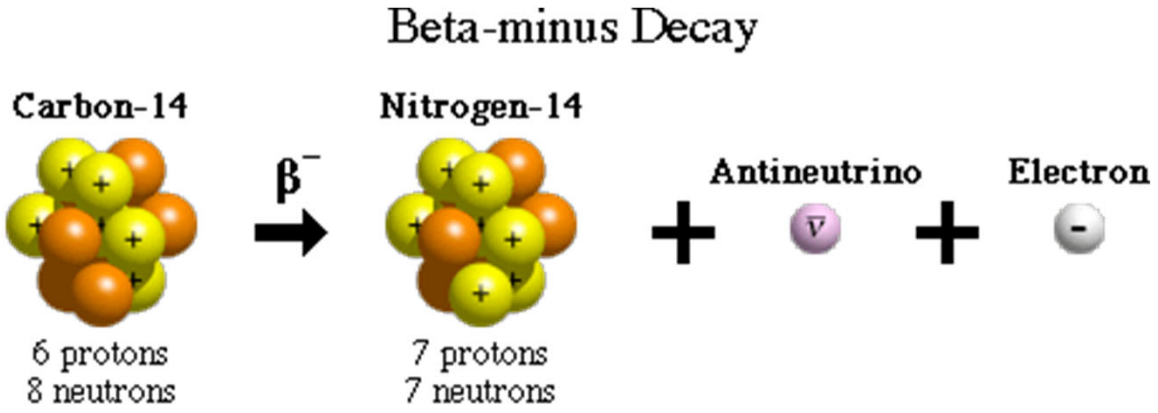

Typical Energy Spectrum of Beta Particles

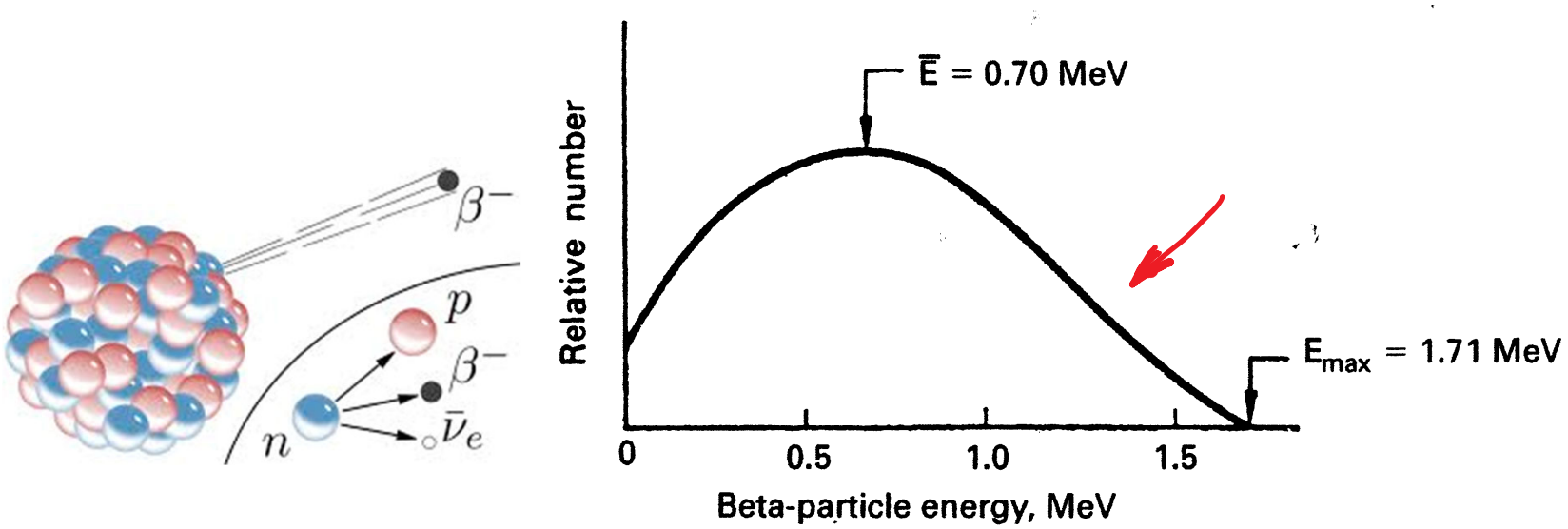

- The energy release is shared by all three daughter products. Due to the relatively large mass of the daughter nucleus, it attains only a small fraction of the energy. Therefore, the kinetic energy of the beta particle is

$$E_{\beta^-} \approx Q - E_{\bar{\nu}}$$

An Example of Cancer Therapy with Radiopharmaceuticals

DIAGNOSIS
68 Gallium-**Octreotate** PET/CT

THERAPY
177 Lutetium-**Octreotate** SPECT-CT

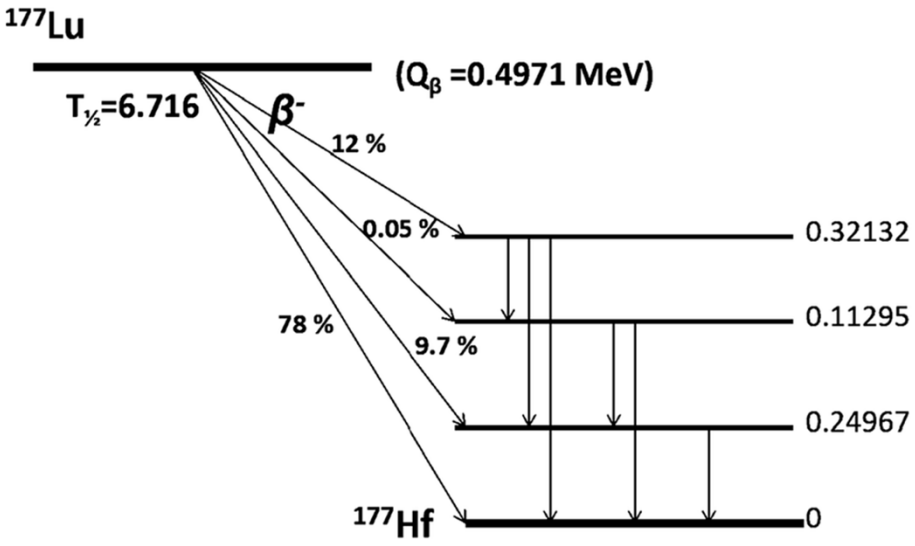

Positron Decay

Positron Decay

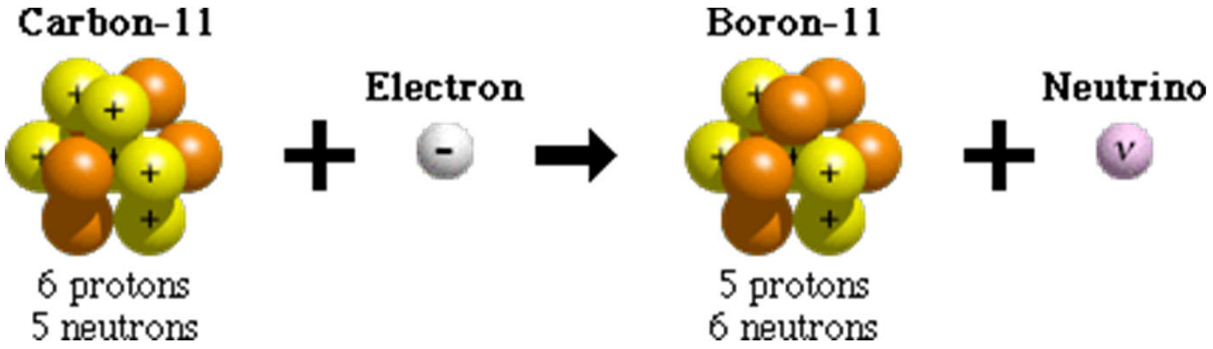

The energy release Q associated with the positron emission process is given by

$$Q \approx M_p - M_d - M_e - M_{e^+} = M_p - (M_d + 2M_e)$$

where the atomic electron binding energy is ignored.

Orbital Electron Capture and Positron Decay

- Electron capture and positron decay are normally competing processes through which a neutron deficient nucleus may attain an increased stability.
- Both the emission of a positron and the capture of an electron, a neutrino is always emitted in order to conserve energy.
- In positron decay, the neutrino carries the difference between the energy release and the energy of the resultant positron. In electron capture, however, the neutrino must be mono-energetic.

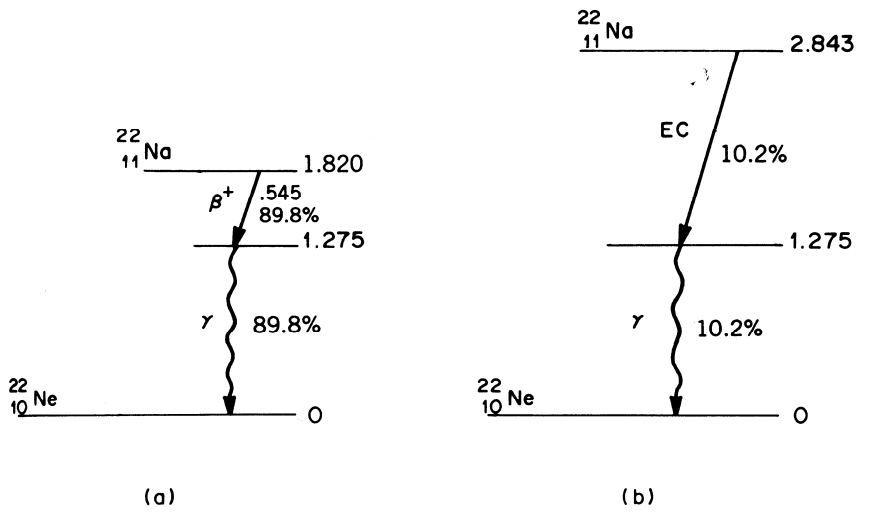

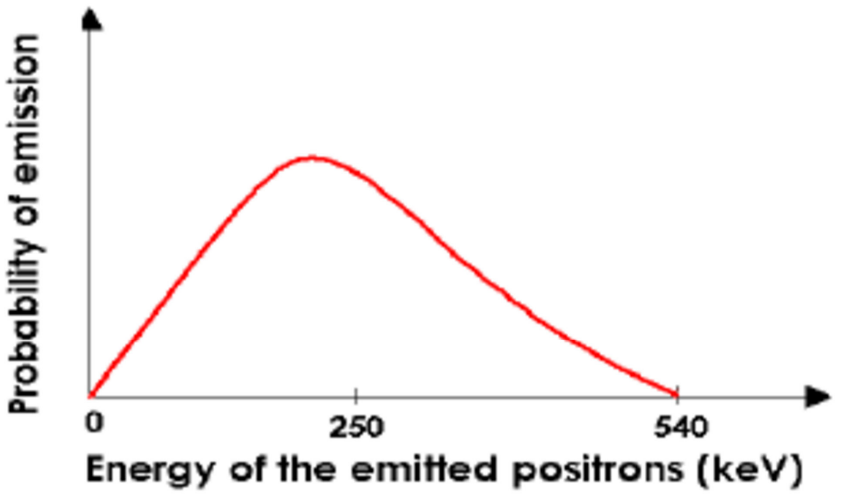

Positron Emission Tomography

Beta-plus decay or positron decay:

$$^{A}_{Z}X \rightarrow {}^{A}_{Z-1}Y + {}^{0}_{1}\beta + \upsilon$$

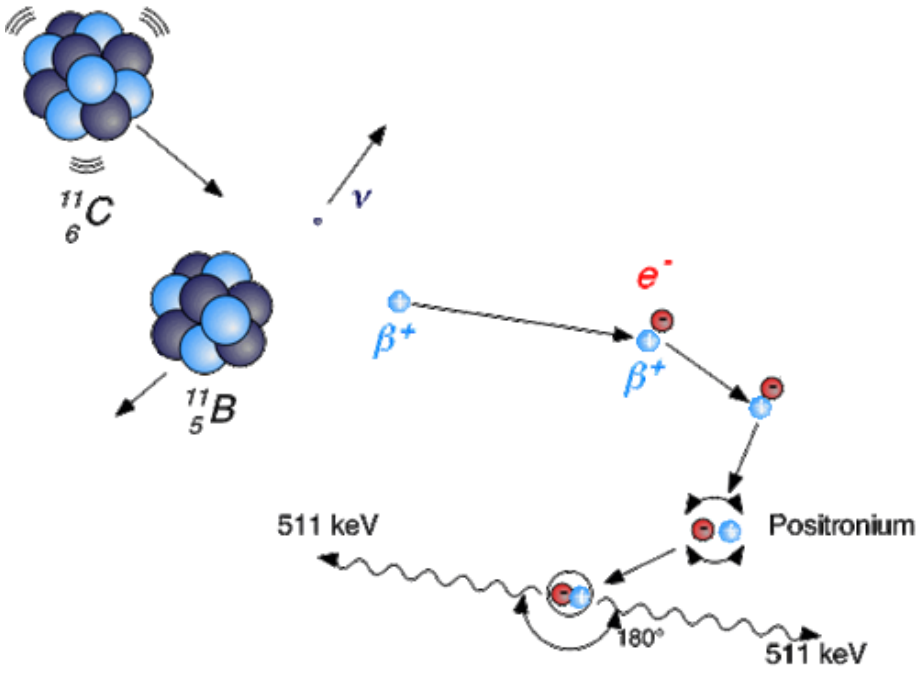

Example of positron annihilation

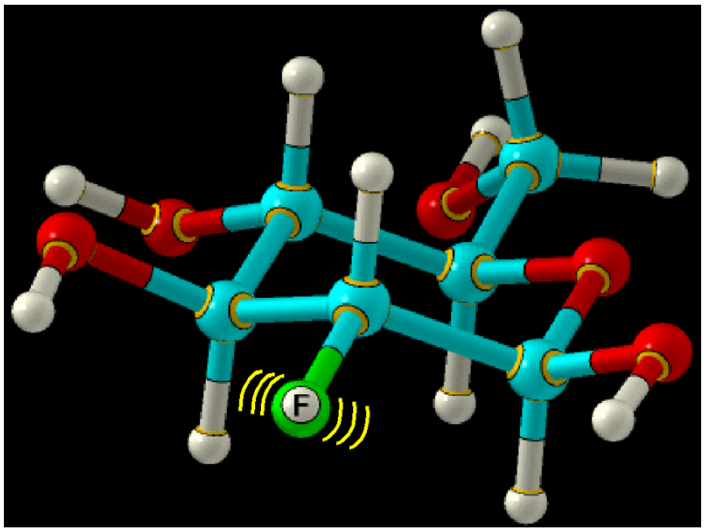

Radiolabeling

What about

- positron range?
- Acollinearity? and …

Positron range in PET imaging: non-conventional isotopes

L Jødal[1], C Le Loirec[2] and C Champion[3]

[1] Department of Nuclear Medicine, Aalborg University Hospital, Aalb
[2] CEA, LIST, F-91191 Gif-sur-Yvette, France
[3] Centre d'Études Nucléaires de Bordeaux Gradignan, CNRS/IN2P3, Bordeaux, Gradignan, France

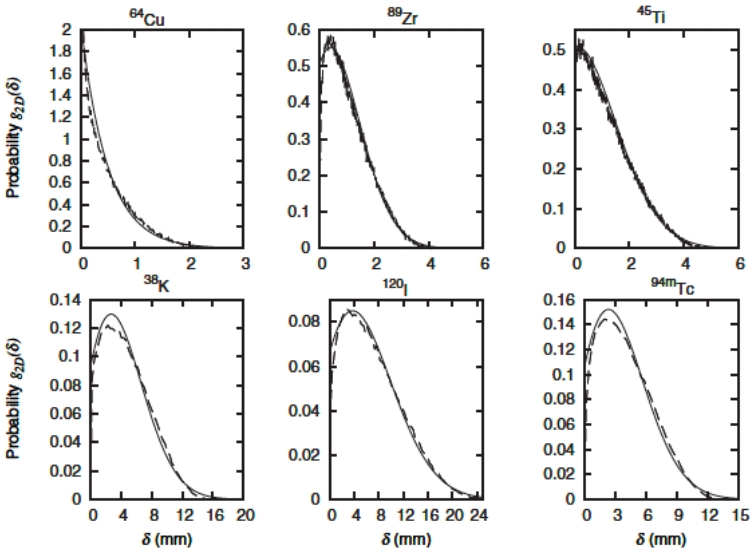

Figure 5. Functions $g_{2D}(\delta)$ obtained from Monte Carlo calculations (broken lines) compared with the expressions defined by (3) using the values of A and B provided in table 2 (smooth lines).

Table 1. Studied isotopes. Values of E_{mean} and E_{max} are determined from the initial spectra used in the Monte Carlo simulations (Le Loirec and Champion 2007a, 2007b, 2007c). Positron ranges have been determined in water.

Isotope	Allowed decay	$T_{½}$	E_{mean} (keV)	E_{max} (keV)	R_{mean} (mm)[a,b]	R_{max} (mm)[a,b]	Example of application
^{64}Cu	Yes, β^+ and β^-	12.7 h	278.2[c]	653.1	0.56	2.9	Detection of small colorectal tumors (Philpott *et al* 1995)
^{22}Na	Yes[d]	2.6 year	220.3	673.5	0.53[e]	2.28[e]	Scanner calibration
^{52}Mn	Yes	5.6 d	244.6	575.8	0.63	2.5	Candidate for bone scanning (Topping *et al* 2013)
^{89}Zr	Yes	78.4 h	402.7	902	1.27	4.2	Quantifying the deposition of monoclonal antibodies in the tissues of tumors (Link *et al* 2006)
^{45}Ti	Yes	3.08 h	442.3	1040.4	1.47	5.2	Uptake measurements to provide insight into the mechanism of the action of titanocene dichloride (Vavere and Welch 2005)
^{51}Mn	Yes	46.2 min	970.2	2185.8	4.3	12.1	Diagnosis and treatment of blood diseases (Sastri *et al* 1981)
^{94m}Tc	Yes	52.0 min	1076.6	2362.9	4.7	12.8	PET substitute for ^{99m}Tc (Liu and Laforest 2007)
^{52m}Mn	Yes	21.1 min	1179	2630	5.3	14.5	Myocardial imaging (Hui *et al* 1979, Daube and Nickles 1985, Tolmachev *et al* 1994)
^{38}K	Yes	7.64 min	1218.8	2728	5.7	15.3	Myocardial perfusion (Bol *et al* 1993)
^{86}Y	No	14.7 h	640	2010.4	2.5	11.1	Uptake measurements prior to therapy using ^{90}Y (Rösch *et al* 1996)
^{124}I	No	4.176 d	825.9	2095	3.4	11.7	Uptake of monoclonal antibodies in solid tumors (Snyder *et al* 1975, Larson *et al* 1992, Daghighian *et al* 1993)
^{120}I	No	81 min	1747	4600	8.3	27	Shorter lifetime and higher positron yield than ^{124}I (Zweit *et al* 1996)

[a] (Le Loirec and Champion 2007b).
[b] (Le Loirec and Champion 2007c).
[c] Mean value for positron emission only.
[d] Decay to the ground state of ^{22}Ne is forbidden ($3^+ \rightarrow 0^+$); instead, nearly 100% of the decays are to an excited state, ^{22}Na (3^+) → ^{22}Ne* (2^+) (Lederer *et al* 1967).
[e] (Le Loirec 2007).

A Few Details on Positron Decay and Their Implications to PET

Isotope	half-life (min)	Maximum positron energy (MeV)	Positron range in water (FWHM in mm)	Production method
^{11}C	20.3	0.96	1.1	cyclotron
^{13}N	9.97	1.19	1.4	cyclotron
^{15}O	2.03	1.70	1.5	cyclotron
^{18}F	109.8	0.64	1.0	cyclotron
^{68}Ga	67.8	1.89	1.7	generator
^{82}Rb	1.26	3.15	1.7	generator

Table 2. Properties of commonly used positron emitting radio-isotopes

- element of life.

Positron Decay and PET Imaging

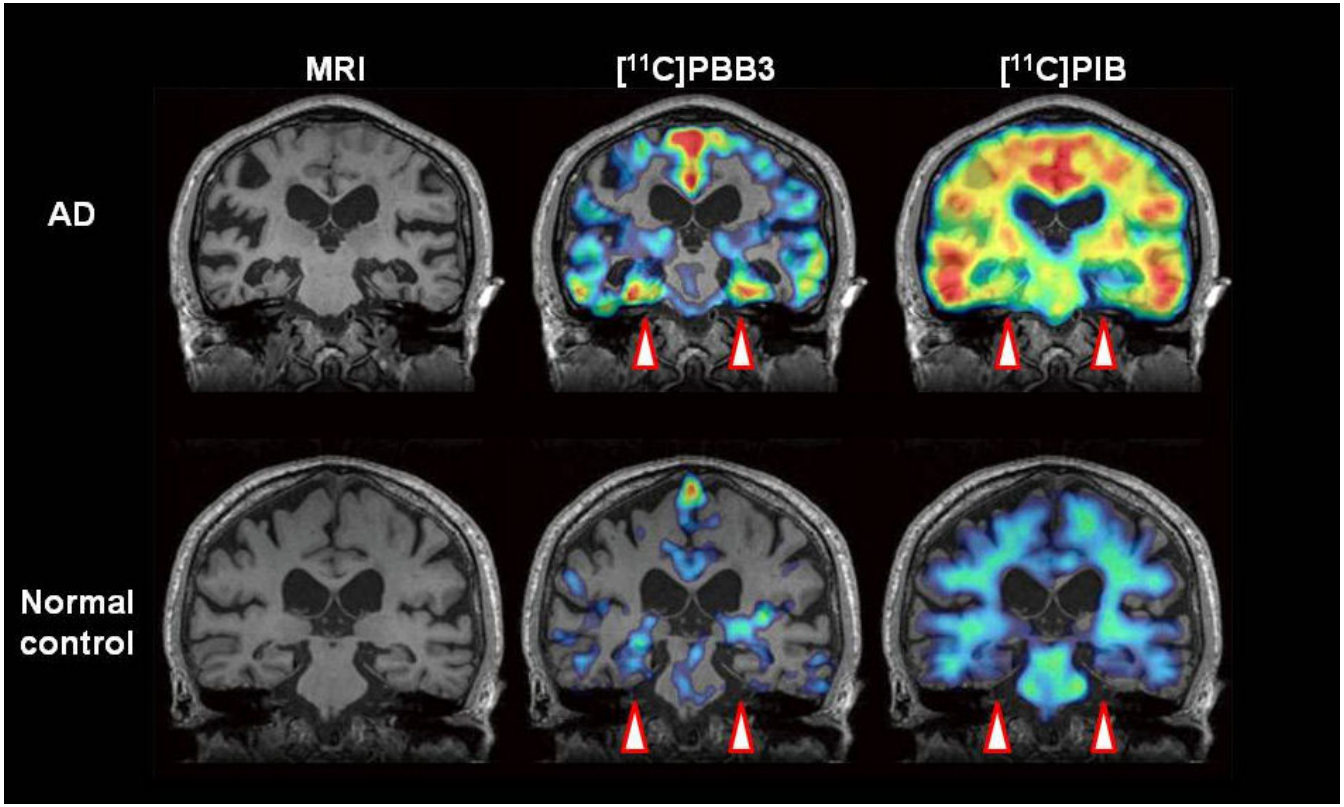

Negative and positive [C-11]PiB PET images. [C-11]PiB PET images taken in the axial plane at levels indicated in the sagittal MRI image at the far left. The scans in the top row illustrate the 79-year-old [C-11]PiB(−) DLB subject that is the focus of the current study. There is no evidence of [C-11]PiB retention except for nonspecific retention in the white matter. The scans in the bottom row illustrate a 65-year-old [C-11]PiB(+) AD subject showing high [C-11]PiB retention throughout the neocortex and the striatum

What is [^{18}F]FDG?

GENERAL INFORMATION

Chemical name of **[^{18}F]FDG** is [^{18}F]-2-Fluoro-2-deoxy-β-D-glucopyranose, Chemical Abstract Service registry number 63503-12-8. More commonly it is called [^{18}F]Fluorodeoxyglucose or simply FDG.

This compound is a radioactive derivative of 2-deoxy-D-glucose labelled with positron-emitting isotope $^{18}_{9}$F in the position 2 of the glucose core structure.

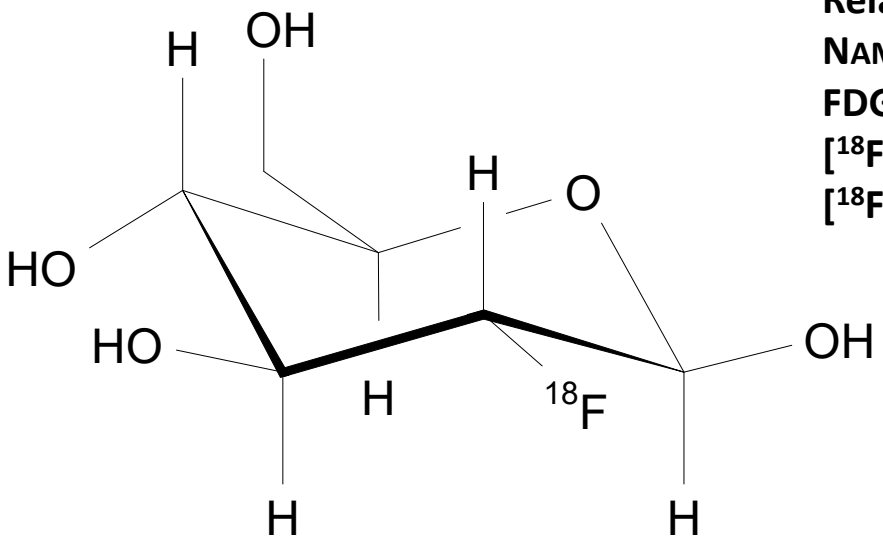

Relative molecular mass: 181.15 g/mol

NAMES:

FDG

[^{18}F]FLUORODEOXYGLUCOSE

[^{18}F]-2-Fluoro-2-deoxy-β-D-glucopyranose

For more details please refer to review article on radiohalogenated sugars.

Functional Imaging with Tremendous Sensitivity Under In Vivo Settings

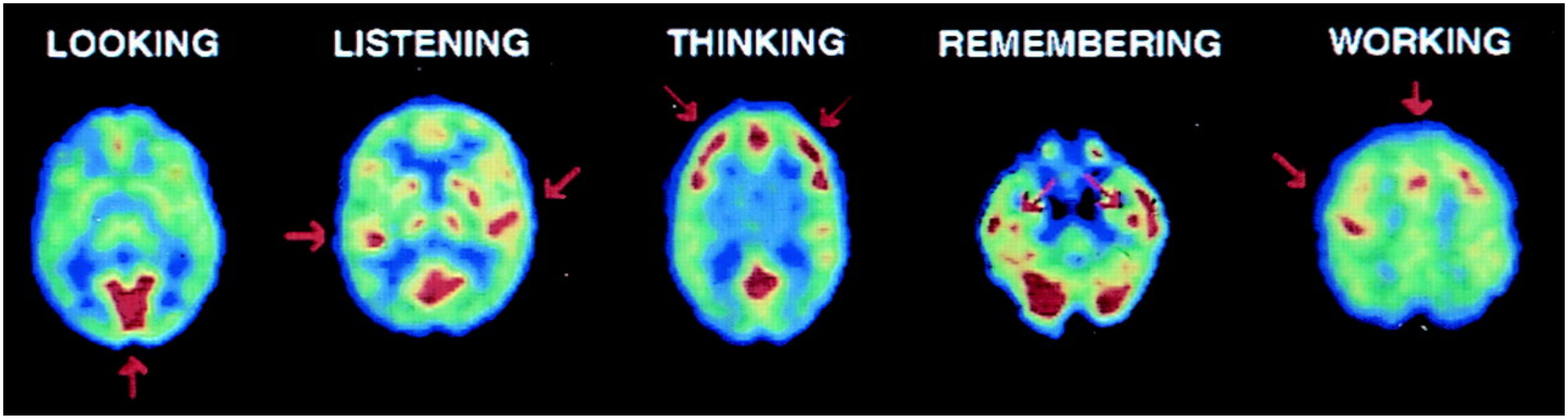

PET studies of glucose metabolism to map human brain's response in performing different tasks.

Michael E. Phelps, "Positron emission tomography provides molecular imaging of biological processes", PNAS, 2000.

PET-labeled probes for biological imaging: (from S. Cherry, UC Davis)

hemodynamic parameters ($H_2{}^{15}O$, ^{15}O-butanol, ^{11}CO, $^{13}NH_3$.....), substrate metabolism(^{18}F-FDG, $^{15}O_2$, ^{11}C-palmitic acid....) protein synthesis (^{11}C-leucine, ^{11}C-methionine, ^{11}C-tyrosine), enzyme activity (^{11}C-deprenyl, ^{18}F-deoxyuracil...), drugs (^{11}C-cocaine, ^{13}N-cisplatin, ^{18}F-fluorouracil...), receptor affinity (^{11}C-raclopride, ^{11}C-carfentanil, ^{11}C-scopalamine), neurotransmitter biochemistry (^{18}F-fluorodopa, ^{11}C-ephedrine...), gene expression (^{18}F-penciclovir, ^{18}F-antisense oligonucleotides) ……

Electron Capture

Energy Release Through Orbital Electron Capture

For positron decay to be possible, we need

$$Q = M_p - M_d - M_e - M_{e^+} > 0,$$

so

$$M_p > M_d + M_e + M_{e^+} = M_d + 2M_e$$

M_p and M_d are the atomic masses of the parent and daughter atoms

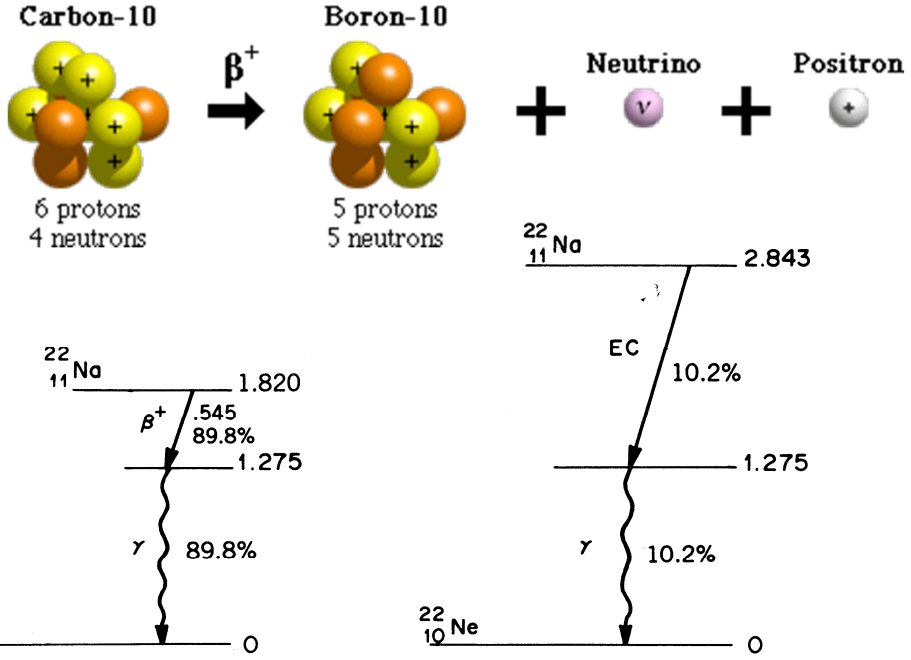

For Electron Capture to occur,

$$Q = M_p - M_d - \phi > 0$$

so that

$$M_p > M_d + \phi$$

where ϕ is the binding energy of the orbital electron

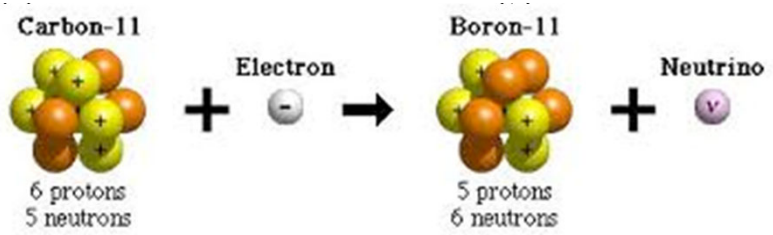

Internal Conversion

- Conversion electrons can originate from several different electron shells within the atom, a single excited state generally leads to several groups of electrons with different energies.
- The only practical laboratory scale source of mono-energetic electron groups in high keV to MeV energy range.

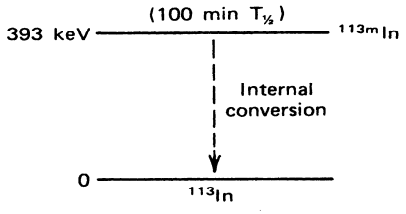

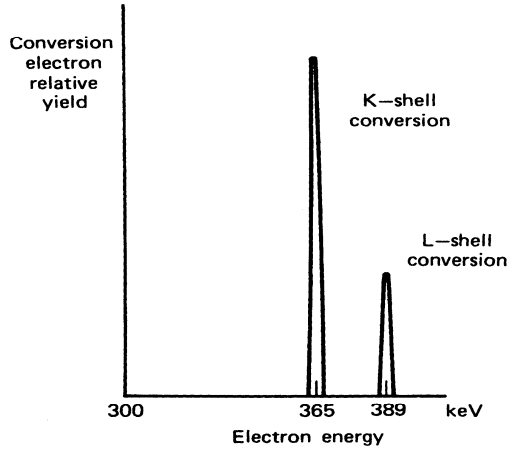

Auger Electrons

- The excitation energy of the atom may be transferred to one of the outer electrons, causing it to be ejected from the atom.
- Auger electrons are roughly the analogue of internal conversion electrons when the excitation energy originates in the atom rather than in the nucleus.

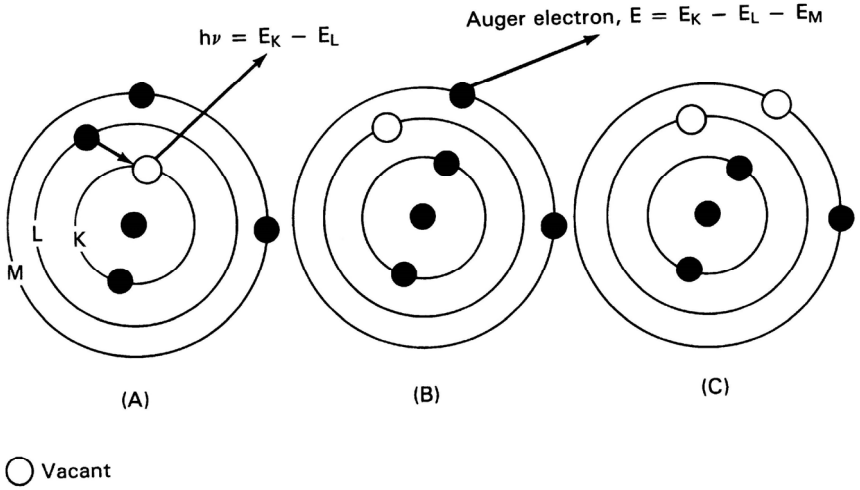

Figure 3.7 (A) The usual emission of a K characteristic X-ray, $h\nu$, energy equal to $E_K - E_L$, the difference in binding energy for the two orbital electrons, K and L. (B) $h\nu$ has been absorbed and a monoenergetic Auger electron is emitted, in the example shown, from the M shell, the energy of which is $E_K - E_L - E_M$. (C) In its final state the atom has vacancies in the L and M orbitals.

Special SPECT Imaging Applications: Single Photon Emission Microscopy

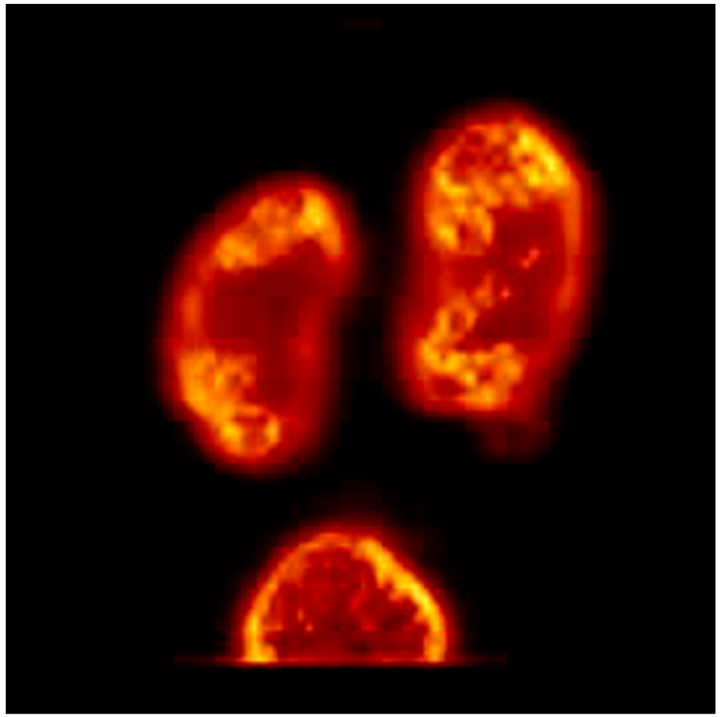

Imaging of mouse kidney I-125, Data from Center for Gamma Ray Imaging, University of Arizona

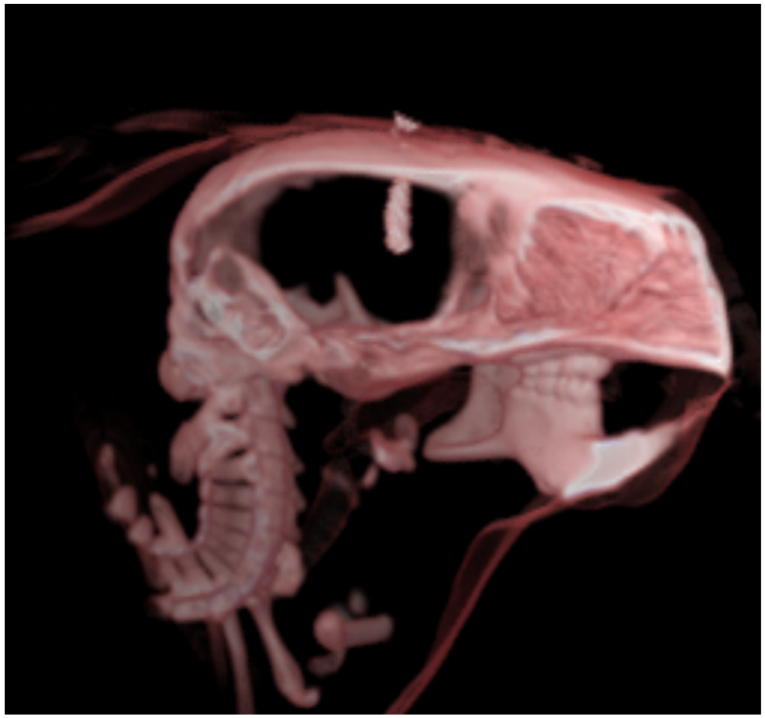

In vivo imaging of (~1500) radiolabeled T cells labeled with I-125 in mouse brain using SPECT (Meng, 2009).

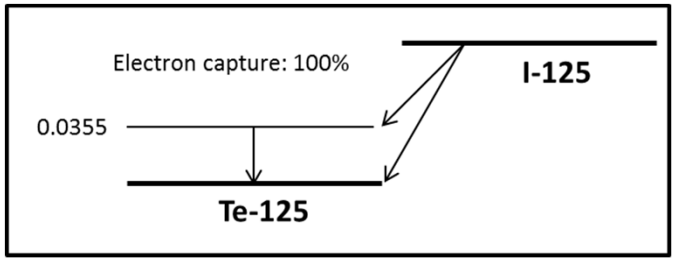

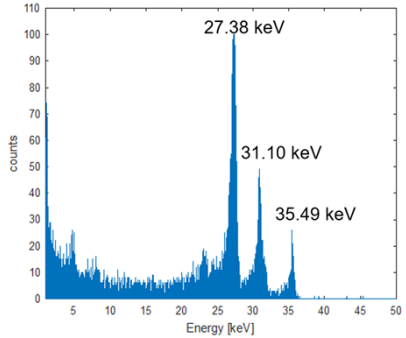

What would be an ideal gamma ray emitter for nuclear imaging?

- Reasonably penetrative…
- Half-life comparable to the biological process we are trying to visualize…
- Easy radiochemistry…
- Biologically safe…
- Clean …

Metastable Nuclear States and Gamma Ray Emission

The lifetimes of nuclear excited states vary, but $\sim 10^{-10}$ s can be regarded as typical. Thus, gamma rays are usually emitted quickly after radioactive decay to an excited daughter state.

In some cases, however, selection rules prevent photon emission for an extended period of time. The excited state of $^{137}_{56}\mathrm{Ba}$ following the decay of $^{137}_{55}\mathrm{Cs}$ has a half-life of 2.55 min. Such a long-lived nuclear state is termed *metastable* and is designated by the symbol m: $^{137m}_{56}\mathrm{Ba}$.

Another example of a metastable nuclide is $^{99m}_{43}\mathrm{Tc}$, which results from the beta decay of the molybdenum isotope $^{99}_{42}\mathrm{Mo}$.
an isomeric transition (IT) to the ground

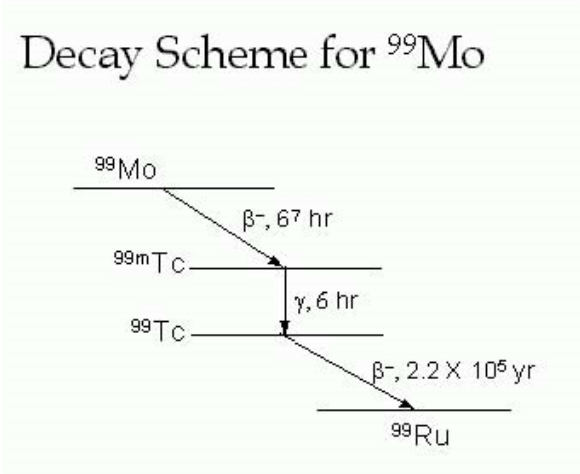

Metastable Nuclear States and Gamma Ray Emission

The lifetimes of nuclear excited states vary, but $\sim 10^{-10}$ s can be regarded as typical. Thus, gamma rays are usually emitted quickly after radioactive decay to an excited daughter state.

In some cases, however, selection rules prevent photon emission for an extended period of time. The excited state of $^{137}_{56}\mathrm{Ba}$ following the decay of $^{137}_{55}\mathrm{Cs}$ has a half-life of 2.55 min. Such a long-lived nuclear state is termed *metastable* and is designated by the symbol m: $^{137\mathrm{m}}_{56}\mathrm{Ba}$.

Another example of a metastable nuclide is $^{99\mathrm{m}}_{43}\mathrm{Tc}$, which results from the beta decay of the molybdenum isotope $^{99}_{42}\mathrm{Mo}$.
an isomeric transition (IT) to the ground

Tc-99m Sestamibi Myocardial Perfusion Imaging (MPI)

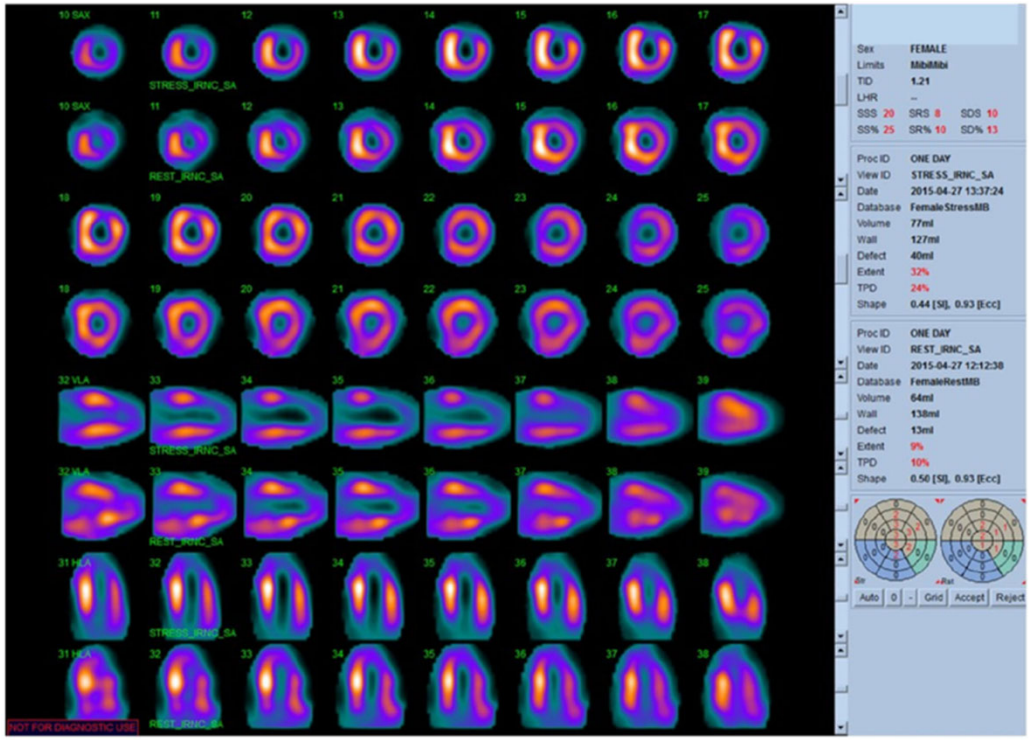

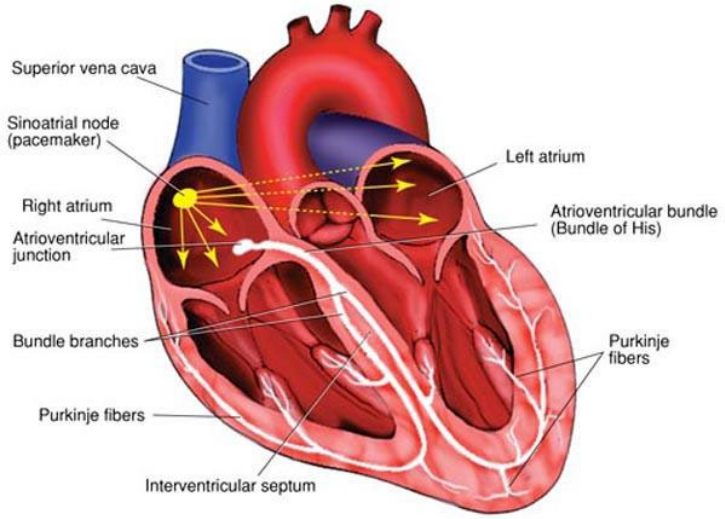

Exercise stress Tc-99m Sestamibi single day myocardial perfusion SPECT images of the female patient with a significant (80%) distal left main coronary artery disease. Classic features of the high-risk scan are present: severe partially reversible perfusion defect, involvement of the LAD and LCX territory, visual transient ischemic dilation and abnormal TID ratio (1.21). The patient presented with symptoms of stable atypical angina. No significant ECG or hemodynamic changes were noted during the stress portion of the test.

https://www.researchgate.net/figure/Exercise-stress-Tc-99m-Sestamibi-single-day-myocardial-perfusion-SPECT-images-of-the_fig1_283448406

What do MPI images look like?

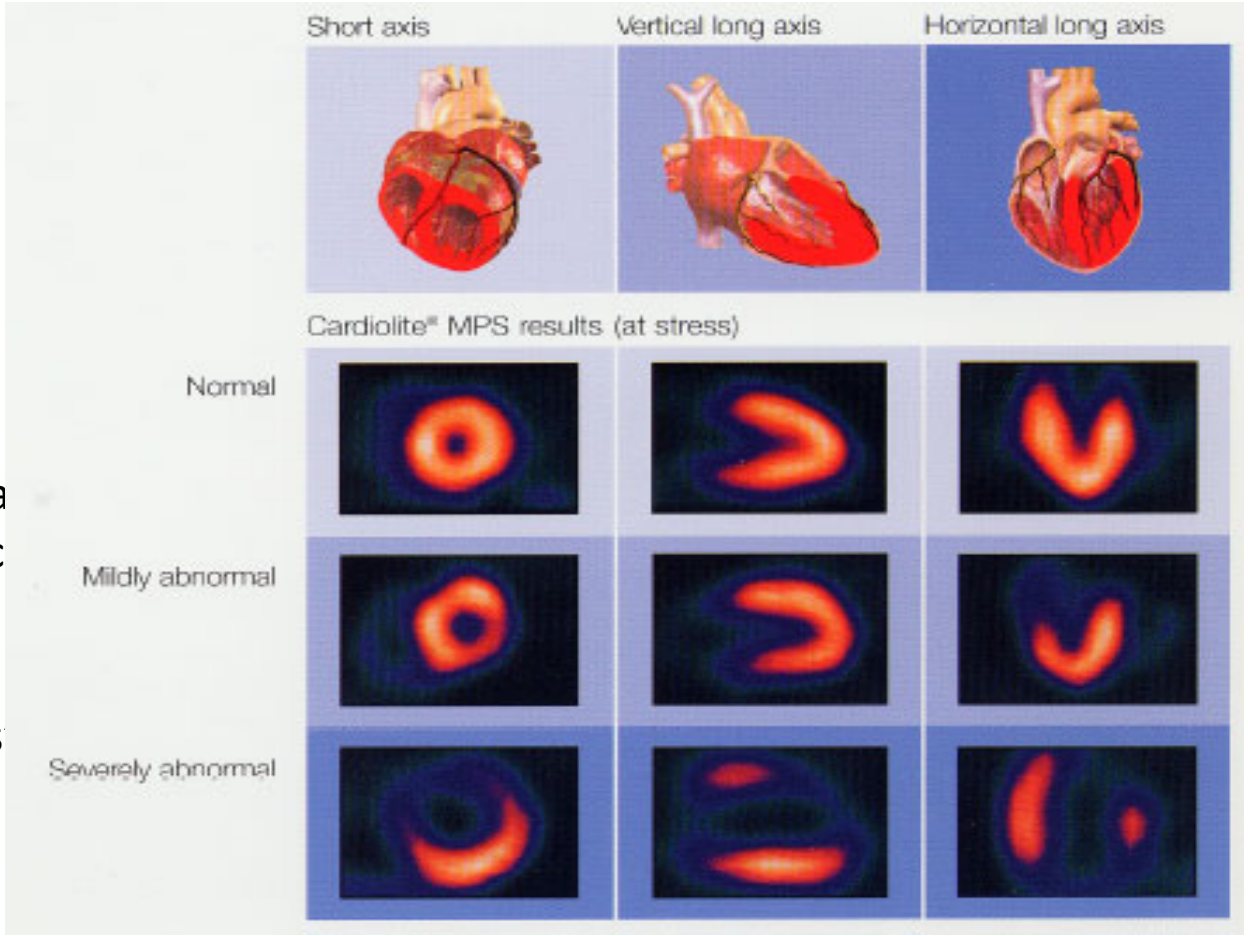

In a typical nuclear cardia
imaging exam, the physic
reviews:

- Static "Summed Perfusion Images
- Dynamic "Gated Images"

Perfusion Images are viewed in three orientations:
SA – Short Axis
VLA – Vertical Long Axis
HLA - Horizontal Long Axis

Therapeutic Beta Emitters

Common isotopes used in nuclear medicine [9][10]

isotope	symbol	Z	$T_{1/2}$	decay	gamma (keV)	positron (keV)
Imaging:						
fluorine-18	^{18}F	9	109.77 m	β^+	511 (193%)	249.8 (97%)[11]
gallium-67	^{67}Ga	31	3.26 d	ec	93 (39%), 185 (21%), 300 (17%)	-
krypton-81m	^{81m}Kr	36	13.1 s	IT	190 (68%)	-
rubidium-82	^{82}Rb	37	1.27 m	β^+	511 (191%)	3.379 (95%)
nitrogen-13	^{13}N	7	9.97 m	β^+	511 (200%)	1190 (100%)[12]
technetium-99m	^{99m}Tc	43	6.01 h	IT	140 (89%)	-
indium-111	^{111}In	49	2.80 d	ec	171 (90%), 245 (94%)	-
iodine-123	^{123}I	53	13.3 h	ec	159 (83%)	-
xenon-133	^{133}Xe	54	5.24 d	β^-	81 (31%)	0.364 (99%)
thallium-201	^{201}Tl	81	3.04 d	ec	69–83* (94%), 167 (10%)	-
Therapy:						
yttrium-90	^{90}Y	39	2.67 d	β^-	-	2.280 (100%)
iodine-131	^{131}I	53	8.02 d	β^-	364 (81%)	0.807 (100%)

Z = atomic number, the number of protons; $T_{1/2}$ = half-life; decay = mode of decay

photons = principle photon energies in kilo-electron volts, keV, (abundance/decay)

β = beta maximum energy in mega-electron volts, MeV, (abundance/decay)

β^+ = β^+ decay; β^- = β^- decay; IT = isomeric transition; ec = electron capture

* X-rays from progeny, mercury, Hg

Therapeutic Beta Emitters

Table 1 - Physical and nuclear characteristics of bone-seeking therapeutic radionuclides[1]

	Maximum energy (MeV)	Average energy (MeV)	Average Range (mm)	T_{half} (days)	yphoton (MeV)
Strontium-89	1.46	0.58	2.4	50.5	None
Phosphorus-32	1.71	0.70	3.0	14.3	None
Tin-117m	0.13[2] 0.15[2]	--- ---	0.22 0.29	14.0	0.159 (86%)
Erbium-169	0.34	0.11	0.30	9.3	None
Lutetium-177	0.50	0.14	0.35	6.7	0.208 (11%)
Rhenium-186	1.08	0.33	1.05	3.7	0.137 (9%)
Samarium-153	0.81	0.22	0.55	1.9	0.103 (29%)
Holmium-166	1.84	0.67	3.3	1.1	0.081 (6%)
Rhenium-188	2.12	0.64	3.8	0.71	0.155 (10%)

[1]Arranged in order of decreasing half-life
[2]Conversion electrons with discrete energies (and range).

Examples for Beta Decay

- Complicated decay schemes and the emission of other particles such as gamma rays.
- Pure beta emitters: ^{3}H, ^{14}C, ^{32}P and ^{90}Sr.

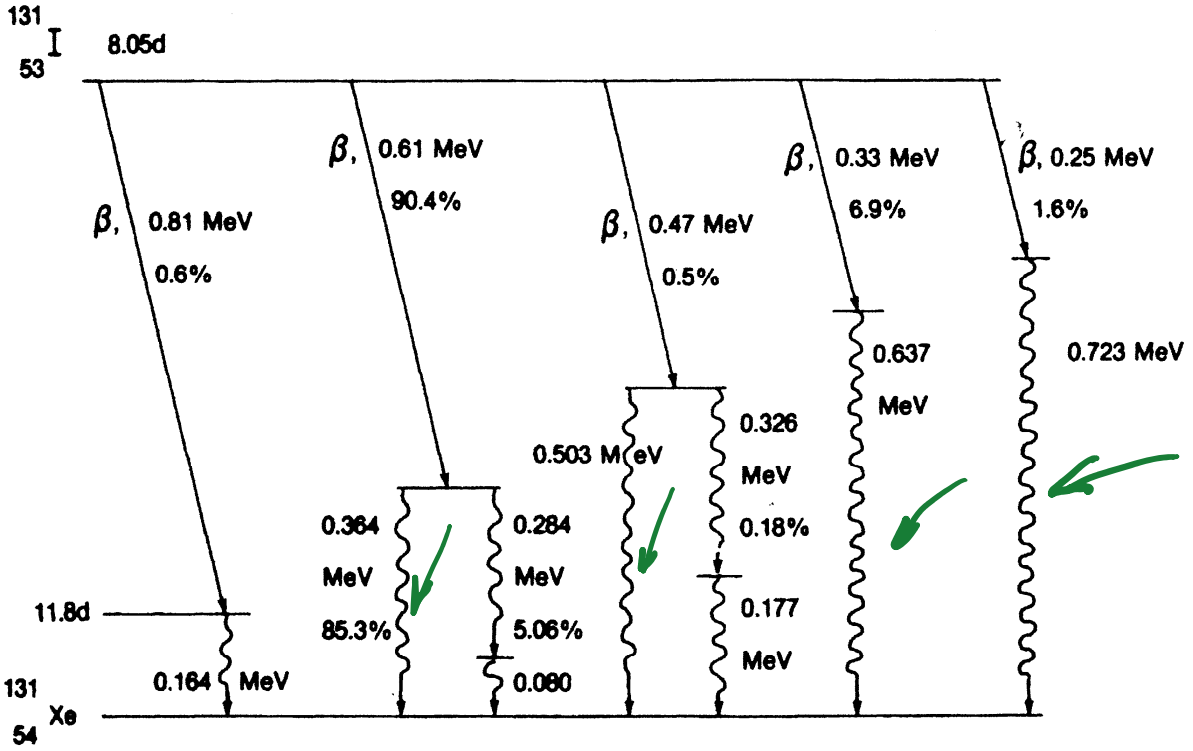

FIGURE 4.7. Iodine-131 transformation (decay) scheme.

I-131 Whole Body Imaging

Differentiation between malignancy and benign changes with SPECT/CT in a patient with
thyroid cancer who underwent 131I whole-body imaging to assess for residual recurrent disease. **Anterior(a)** and **posterior (b)** 131I scans show focal activity in the right suprarenal region.

Coronal (c) and **axial (d)** SPECT/CT images show that the uptake is located in the renal collecting system (arrow),consistent with physiologic urinary activity, and not recurrence of disease.

www.lancastergeneralhealth.org/LGH/ECommerceSite/

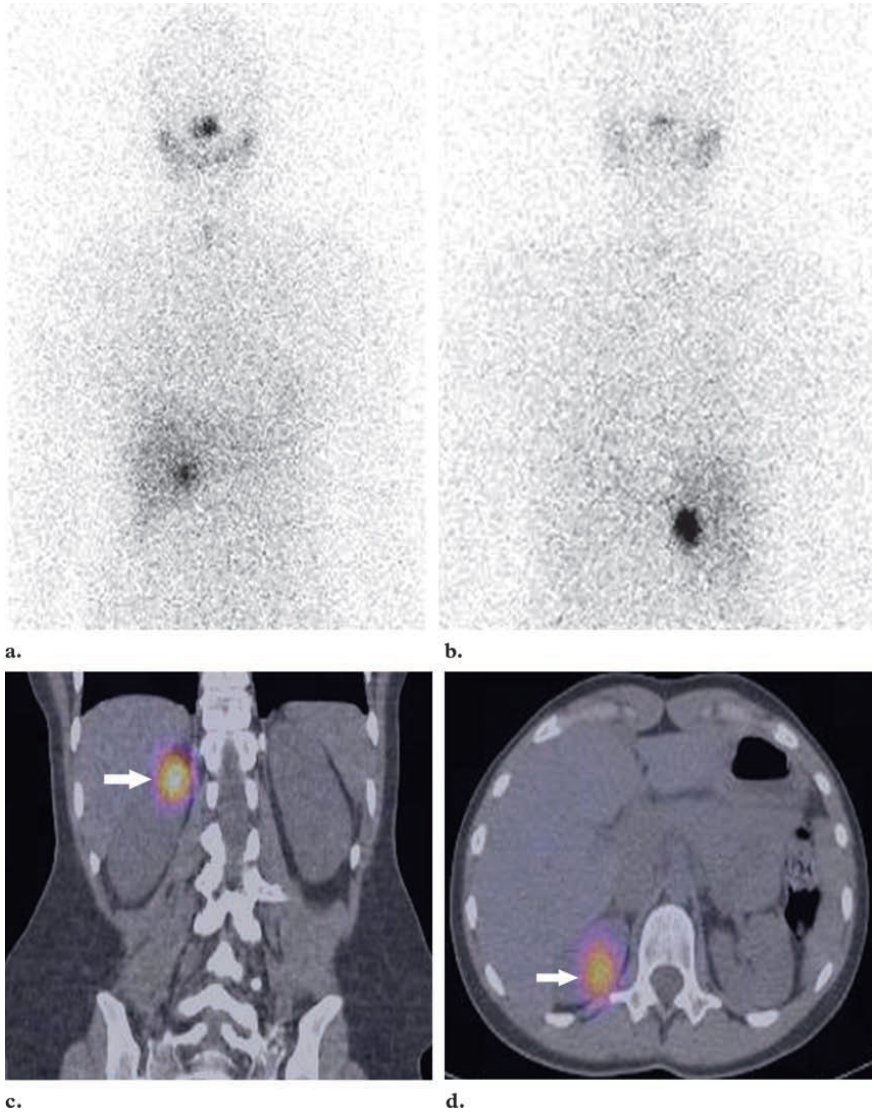

Case Report: “Management of metastatic thyroid cancer in pregnancy: risk and uncertainty”, by Christopher W Rowe et al., Endocrinology, Diabetes and Metabolism, 2016

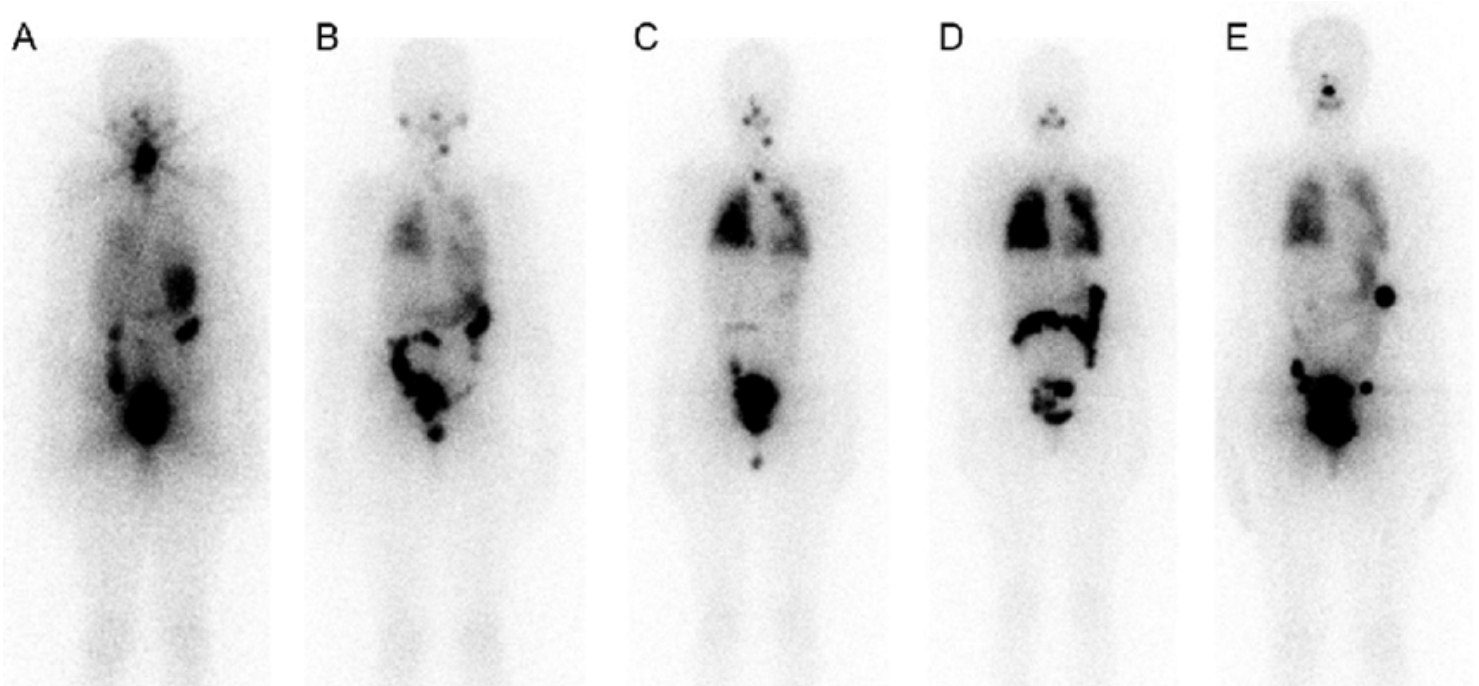

Serial post-I 131 therapy scans (anterior whole body views). (A) Age 10, 3.01 GBq; (B) age 11, 2.95 GBq; (C) age 13, 4.3 GBq; (D) age 14, 5.1 GBq; (E) age 15, 9.9 GBq, 7 months before conception. Neck disease present at age 13 (C) was treated surgically. The final study (E) showed the presence of radioiodine avid bilateral pulmonary metastases (<5 mm maximum diameter on computed tomography) and very small, low-grade lower neck disease. The focal uptake in the left upper abdomen is colonic and is likely physiological in nature.

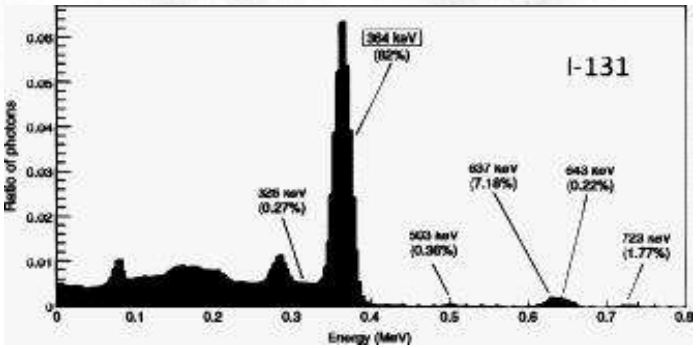

^{225}Ac-PSMA-617 for PSMA-Targeted α-Radiation Therapy of Metastatic Castration-Resistant Prostate Cancer

Clemens Kratochwil*[1], Frank Bruchertseifer*[2], Frederik L. Giesel[1], Mirjam Weis[2], Frederik A. Verburg[3], Felix Mottaghy[3], Klaus Kopka[4], Christos Apostolidis[2], Uwe Haberkorn[1], and Alfred Morgenstern[2]

[1]Department of Nuclear Medicine, University Hospital Heidelberg, Heidelberg, Germany; [2]European Commission, Joint Research Centre, Institute for Transuranium Elements, Karlsruhe, Germany; [3]Department of Nuclear Medicine, RWTH University Hospital Aachen, Aachen, Germany; and [4]Division of Radiopharmaceutical Chemistry, German Cancer Research Center, Heidelberg, Germany

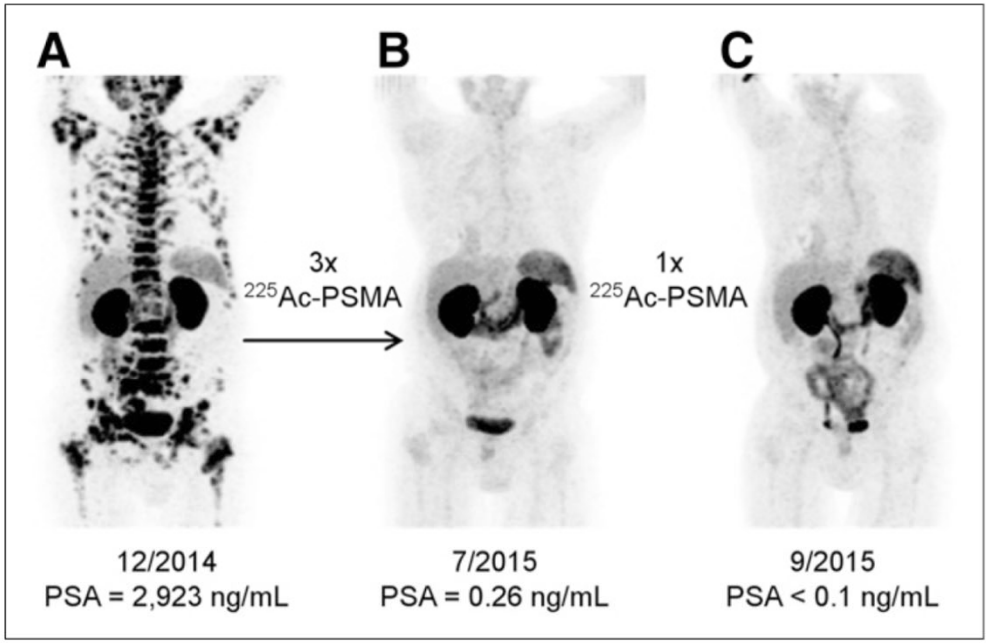

FIGURE 1. ^{68}Ga-PSMA-11 PET/CT scans of patient A. Pretherapeutic tumor spread (A), restaging 2 mo after third cycle of ^{225}Ac-PSMA-617 (B), and restaging 2 mo after one additional consolidation therapy (C).

Hyperspectral SPECT Imaging of TAT

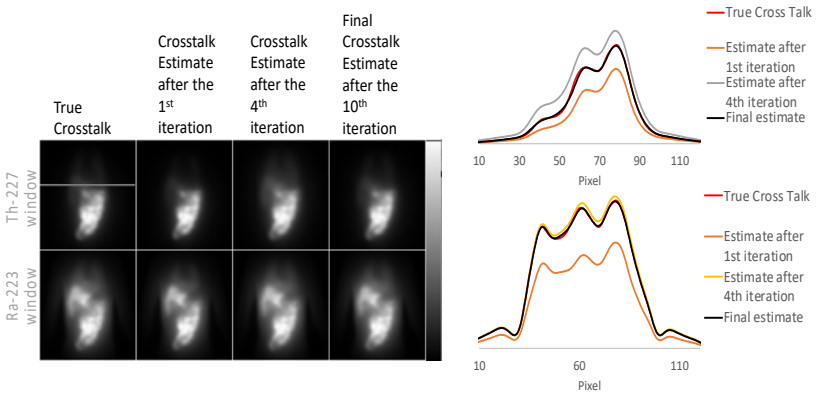

Estimated crosstalk of Th227/Ra223 imaging.

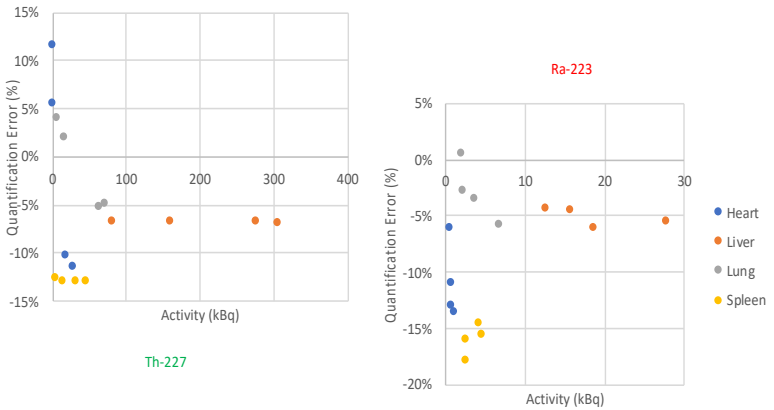

VOI quantification. Left: Th-227; Right: Ra-223.

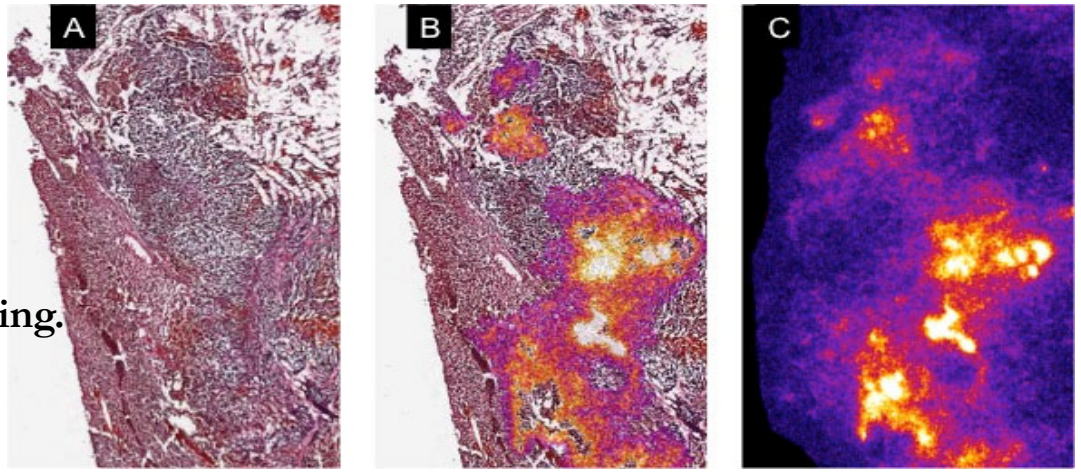

H&E staining of VX2 tumor and surrounding liver section (A) and corresponding α-Camera image (C) 3 hours post-injection of ^{225}Ac-DOTAGA-TDA. (B) Merged image showing segmented high-intensity regions overlayed on H&E stained slide. Segmented regions do not exactly match the tumor boundaries due to differences in tissue processing and because the comparison is made across two different 12-μm-thick sections.

Data presented in this slide is kindly provided by our collaborators, Dr. Eric Frey and Dr. Yong Du at Johns Hopkins Medical School

Atomic Emissions

Energy Release of Orbital Electron Capture

For Positron Decay to be possible, we need

$$Q = M_p - M_d - M_e - M_{e^+} > 0,$$

so

$$M_p > M_d + M_e + M_{e^+} = M_d + 2M_e$$

M_p and M_d are the atomic masses of the parent and daughter atoms

For Electron Capture to occur,

$$Q = M_p - M_d - \phi > 0$$

so that

$$M_p > M_d + \phi$$

where ϕ is the binding energy of the orbital electron

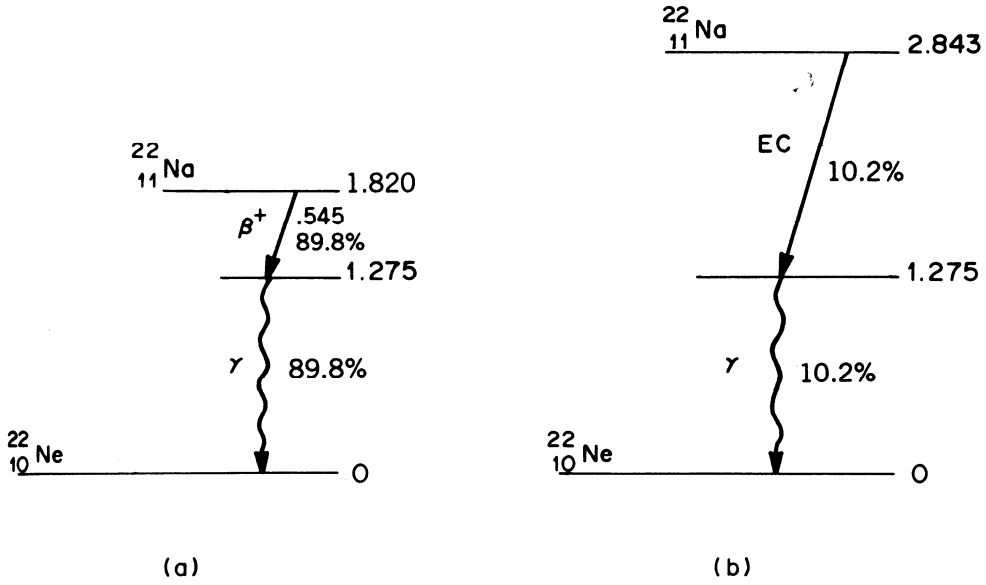

Internal Conversion

Begins with an excited nuclear state

De-excite through the emission of a gamma ray

The excitation energy is transferred directly to an orbital electron, causing it to be ejected from the atom

$$E_{\beta^-} = E_{ex} - E_b$$

Conversion electron with an energy

$$\text{IC Coefficient (or Branching Ratio)} = \frac{N_\gamma}{N_e}$$

Auger Electrons and Characteristic X-rays

- The excitation energy of the atom may be transferred to one of the outer electrons, causing it to be ejected from the atom.
- Auger electrons are roughly the analogue of internal conversion electrons when the excitation energy originates in the atom rather than in the nucleus.

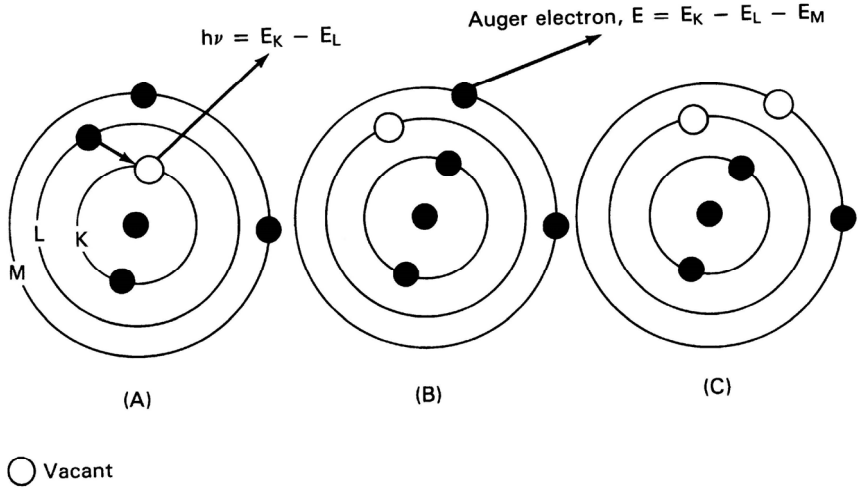

Figure 3.7 (A) The usual emission of a K characteristic X-ray, $h\nu$, energy equal to $E_K - E_L$, the difference in binding energy for the two orbital electrons, K and L. (B) $h\nu$ has been absorbed and a monoenergetic Auger electron is emitted, in the example shown, from the M shell, the energy of which is $E_K - E_L - E_M$. (C) In its final state the atom has vacancies in the L and M orbitals.

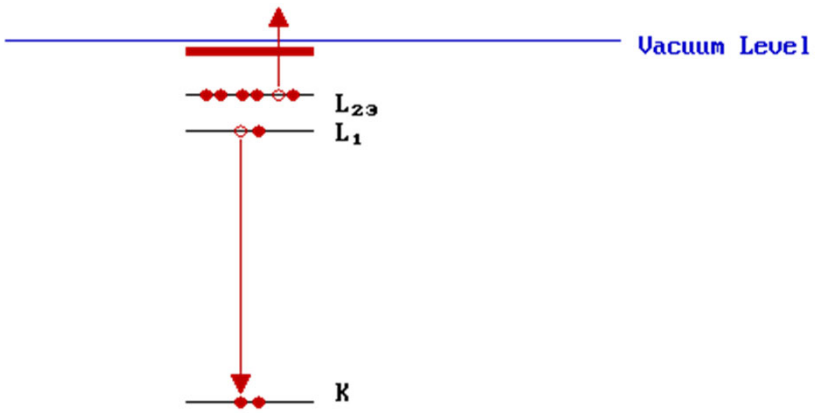

$$E_{a.e.} = (E_K - E_{L_1}) - E_{L_{23}}$$

Examples of Radioactivity from Medical Radioisotopes

http://www.nucleide.org/DDEP_WG/Nuclides/I-123_tables.pdf
http://www.nucleide.org/DDEP_WG/Nuclides/I-131_tables.pdf

$^{123}_{53}\mathrm{I}_{70}$

1 Decay Scheme

I-123 disintegrates by electron capture mainly via the 159 keV level of Te-123 (97%).

L' iode123 se désintègre par capture électronique principalement vers le niveau excité de 159 keV du tellure 123, avec une probabilité de 97%.

2 Nuclear Data

$T_{1/2}(^{123}\mathrm{I})$	:	13,2234	(37)	h
$T_{1/2}(^{123}\mathrm{Te})$	:	12		10^{12} a
$Q^+(^{123}\mathrm{I})$	:	1234	(3)	keV

2.1 Electron Capture Transitions

	Energy keV	Probability × 100	Nature	lg ft	P_K	P_L	P_M
$\epsilon_{0,13}$	165,8 (30)	0,0079 (4)	Allowed	7,59	0,8082 (21)	0,1503 (15)	0,0336 (7)
$\epsilon_{0,12}$	197,4 (30)	0,0025 (9)	Allowed	8,27	0,8182 (18)	0,1427 (13)	0,0316 (6)
$\epsilon_{0,11}$	237,9 (30)	0,0035 (3)	1st Forbidden	8,31	0,8266 (16)	0,1363 (12)	0,0300 (6)
$\epsilon_{0,10}$	339,3 (30)	0,0744 (13)	Allowed	7,32	0,8377 (15)	0,1283 (11)	0,0278 (5)
$\epsilon_{0,9}$	450,4 (30)	0,1461 (20)	Allowed	7,29	0,8436 (14)	0,1237 (10)	0,0267 (5)
$\epsilon_{0,8}$	464,7 (30)	0,0037 (6)	Allowed	8,92	0,8441 (14)	0,1233 (10)	0,0266 (5)
$\epsilon_{0,7}$	536,5 (30)	0,419 (13)	Allowed	6,98	0,8464 (14)	0,1216 (10)	0,0262 (5)
$\epsilon_{0,6}$	546 (3)	1,40 (12)	Allowed	6,49	0,8466 (14)	0,1214 (10)	0,0261 (5)
$\epsilon_{0,4}$	728,7 (30)	0,349 (42)	Allowed	7,35	0,8501 (14)	0,1187 (10)	0,0254 (5)
$\epsilon_{0,3}$	744,3 (30)	0,0025 (10)	Allowed	9,52	0,8503 (14)	0,1186 (10)	0,0254 (5)
$\epsilon_{0,2}$	794 (3)	0,419 (5)	Allowed	7,35	0,8510 (14)	0,1181 (10)	0,0253 (5)
$\epsilon_{0,1}$	1075 (3)	97,18 (32)	Allowed	5,26	0,8533 (14)	0,1163 (10)	0,0248 (5)

2.2 Gamma Transitions and Internal Conversion Coefficients

	Energy keV	$P_{\gamma+ce}$ × 100	Multipolarity	α_K	α_L	α_T
$\gamma_{1,0}$(Te)	158,99 (5)	99,22 (30)	M1 + 1,22%E2	0,1648 (16)	0,02160 (22)	0,1918 (19)
$\gamma_{13,10}$(Te)	174,2 (3)	0,00099 (30)	M1 + 50% E2	0,159 (32)	0,029 (12)	0,195 (47)
$\gamma_{6,4}$(Te)	182,61 (8)	0,021 (6)	M1 + 50% E2	0,138 (24)	0,024 (10)	0,168 (38)
$\gamma_{7,4}$(Te)	192,18 (9)	0,0227 (10)	M1 + 50% E2	0,118 (20)	0,020 (8)	0,143 (30)
$\gamma_{10,7}$(Te)	197,22 (11)	0,00037 (19)	M1 + 50% E2	0,109 (18)	0,018 (7)	0,132 (26)
$\gamma_{6,3}$(Te)	198,25 (12)	0,0040 (8)	M1 + 50% E2	0,107 (17)	0,018 (7)	0,130 (26)
$\gamma_{10,6}$(Te)	206,79 (10)	0,0037 (9)	M1 + 50% E2	0,094 (14)	0,016 (5)	0,114 (21)
$\gamma_{7,3}$(Te)	207,82 (13)	0,00125 (36)	M1 + 50% E2	0,093 (14)	0,015 (5)	0,119 (20)
$\gamma_{6,2}$(Te)	247,96 (8)	0,0743 (25)	M1 + 50% E2	0,054 (5)	0,0084 (21)	0,065 (8)
$\gamma_{7,2}$(Te)	257,52 (9)	0,0017 (2)	E2	0,0526 (16)	0,00917 (27)	0,0640 (19)
$\gamma_{9,4}$(Te)	278,26 (8)	0,0024 (4)	M1 + 50% E2	0,0387 (22)	0,0058 (11)	0,0459 (36)
$\gamma_{2,1}$(Te)	281,03 (7)	0,0822 (10)	M1 + 13,2% E2	0,0362 (20)	0,0048 (11)	0,0422 (33)
$\gamma_{10,5}$(Te)	295,17 (21)	0,001582 (4)				
$\gamma_{8,2}$(Te)	329,38 (18)	0,0026 (6)				
$\gamma_{3,1}$(Te)	330,71 (11)	0,01197 (34)	E2	0,0237 (7)	0,00376 (11)	0,0284 (9)
$\gamma_{9,2}$(Te)	343,73 (8)	0,0044 (3)				
$\gamma_{4,1}$(Te)	346,35 (7)	0,1287 (9)	M1 + 0,49% E2	0,02080 (14)	0,00262 (29)	0,02407 (23)
$\gamma_{10,3}$(Te)	405,04 (14)	0,00298 (23)				
$\gamma_{12,5}$(Te)	437,5 (3)	0,0007 (7)				
$\gamma_{2,0}$(Te)	440,02 (5)	0,4280 (44)	M1 + 81,5% E2	0,0103 (7)	0,001452 (18)	0,0121 (7)
$\gamma_{10,2}$(Te)	454,76 (15)	0,00412 (22)				
$\gamma_{4,0}$(Te)	505,34 (6)	0,268 (42)	M1 + 1% E2	0,0081 (7)	0,001063 (27)	0,0093 (7)
$\gamma_{6,1}$(Te)	528,96 (7)	1,28 (12)				
$\gamma_{7,1}$(Te)	538,54 (8)	0,393 (13)	E2 + 50% M3	0,032 (26)	0,0049 (41)	0,038 (31)
$\gamma_{11,2}$(Te)	556,06 (16)	0,0029 (3)				
$\gamma_{13,4}$(Te)	562,84 (12)	0,00115 (7)				
$\gamma_{13,3}$(Te)	578,48 (20)	0,00126 (8)				
$\gamma_{5,0}$(Te)	599,69 (16)	0,00266 (17)				
$\gamma_{8,1}$(Te)	610,27 (23)	0,0011 (3)				
$\gamma_{9,1}$(Te)	624,61 (7)	0,0802 (20)	M1 + 62,8% E2	0,0042 (5)	0,000549 (40)	0,0049 (6)
$\gamma_{13,2}$(Te)	628,26 (22)	0,00164 (14)				
$\gamma_{6,0}$(Te)	687,95 (10)	0,0269 (6)				
$\gamma_{10,1}$(Te)	735,78 (9)	0,0616 (8)				
$\gamma_{9,0}$(Te)	783,62 (6)	0,0591 (11)				
$\gamma_{11,1}$(Te)	837,1 (2)	0,000582 (8)				
$\gamma_{12,1}$(Te)	877,65 (17)	0,00083 (7)				
$\gamma_{10,0}$(Te)	894,8 (2)	0,00101 (7)				
$\gamma_{13,1}$(Te)	909,19 (12)	0,00141 (8)				
$\gamma_{12,0}$(Te)	1036,64 (17)	0,00097 (7)				
$\gamma_{13,0}$(Te)	1068,18 (15)	0,00142 (7)				

3 Atomic Data

3.1 Te

ω_K	:	0,875	(4)
$\bar{\omega}_L$	:	0,0862	(35)
n_{KL}	:	0,917	(4)

3.1.1 X Radiations

		Energy keV		Relative probability
X_K				
	$K\alpha_2$	27,202		53,7
	$K\alpha_1$	27,4726		100
	$K\beta_3$	30,9446	}	
	$K\beta_1$	30,996	}	
	$K\beta''_5$	31,236	}	28,6
	$K\beta'_5$	31,241	}	
	$K\beta_2$	31,7008	}	
	$K\beta_4$	31,774	}	6,2
	$KO_{2,3}$	31,812	}	
X_L				
	$L\ell$	3,336		
	$L\alpha$	3,76 – 3,77		
	$L\eta$	3,606		
	$L\beta$	4,02 – 4,37		
	$L\gamma$	4,44 – 4,82		

3.1.2 Auger Electrons

	Energy keV	Relative probability
Auger K		
KLL	21,804 – 22,989	100
KLX	25,814 – 27,470	45,3
KXY	29,80 – 31,81	5,13
Auger L	2,3 – 4,8	

4 Electron Emissions

		Energy keV		Electrons per 100 disint.
e_{AL}	(Te)	2,3 - 4,8		95,3 (6)
e_{AK}	(Te)			12,4 (4)
	KLL	21,804 - 22,989	}	
	KLX	25,814 - 27,470	}	
	KXY	29,80 - 31,81	}	
$ec_{1,0\ K}$	(Te)	127,176 (5)		13,72 (14)
$ec_{1,0\ L}$	(Te)	154,051 - 154,649		1,798 (19)

5 Photon Emissions

5.1 X-Ray Emissions

		Energy keV		Photons per 100 disint.	
XL	(Te)	3,336 — 4,82		9,0 (4)	
$XK\alpha_2$	(Te)	27,202		24,69 (20)	} Kα
$XK\alpha_1$	(Te)	27,4726		45,98 (29)	}
$XK\beta_3$	(Te)	30,9446	}		
$XK\beta_1$	(Te)	30,996	}	13,16 (17)	$K'\beta_1$
$XK\beta''_5$	(Te)	31,236	}		
$XK\beta'_5$	(Te)	31,241	}		
$XK\beta_2$	(Te)	31,7008	}		
$XK\beta_4$	(Te)	31,774	}	2,86 (8)	$K'\beta_2$
$XKO_{2,3}$	(Te)	31,812	}		

5.2 Gamma Emissions

	Energy keV	Photons per 100 disint.
$\gamma_{1,0}$(Te)	158,97 (5)	83,25 (21)
$\gamma_{13,10}$(Te)	174,2 (3)	0,00083 (25)

	Energy keV	Photons per 100 disint.
$\gamma_{6,4}$(Te)	182,61 (6)	0,018 (5)
$\gamma_{7,4}$(Te)	192,17 (7)	0,0199 (7)
$\gamma_{10,7}$(Te)	197,22	0,00033 (17)
$\gamma_{6,3}$(Te)	198,23	0,0035 (7)
$\gamma_{10,6}$(Te)	206,79	0,0033 (8)
$\gamma_{7,3}$(Te)	207,8	0,00112 (32)
$\gamma_{6,2}$(Te)	247,96 (5)	0,0698 (23)
$\gamma_{7,2}$(Te)	257,51 (15)	0,0016 (2)
$\gamma_{9,4}$(Te)	278,36 (12)	0,0023 (4)
$\gamma_{2,1}$(Te)	281,03 (5)	0,0789 (9)
$\gamma_{10,5}$(Te)	295,17	0,001582 (4)
$\gamma_{8,2}$(Te)	329,38 (17)	0,0026 (6)
$\gamma_{3,1}$(Te)	330,70 (8)	0,01164 (33)
$\gamma_{9,2}$(Te)	343,73 (14)	0,0044 (3)
$\gamma_{4,1}$(Te)	346,35 (5)	0,1257 (9)
$\gamma_{10,3}$(Te)	405,02 (13)	0,00298 (23)
$\gamma_{12,5}$(Te)	437,5 (3)	0,0007 (7)
$\gamma_{2,0}$(Te)	440,02 (5)	0,4229 (43)
$\gamma_{10,2}$(Te)	454,76 (15)	0,00412 (22)
$\gamma_{4,0}$(Te)	505,33 (5)	0,266 (42)
$\gamma_{6,1}$(Te)	528,96 (5)	1,28 (12)
$\gamma_{7,1}$(Te)	538,54 (5)	0,3788 (43)
$\gamma_{11,2}$(Te)	556,05 (13)	0,0029 (3)
$\gamma_{13,4}$(Te)	562,79 (12)	0,00115 (7)
$\gamma_{13,3}$(Te)	578,26 (20)	0,00126 (8)
$\gamma_{5,0}$(Te)	599,69 (16)	0,00266 (17)
$\gamma_{8,1}$(Te)	610,05 (23)	0,0011 (3)
$\gamma_{9,1}$(Te)	624,57 (5)	0,0798 (20)
$\gamma_{13,2}$(Te)	628,26 (22)	0,00164 (14)
$\gamma_{6,0}$(Te)	687,95 (10)	0,0269 (6)
$\gamma_{10,1}$(Te)	735,78 (7)	0,0616 (8)
$\gamma_{9,0}$(Te)	783,59 (6)	0,0591 (11)
$\gamma_{11,1}$(Te)	837,1 (2)	0,000582 (8)
$\gamma_{12,1}$(Te)	877,52 (17)	0,00083 (7)
$\gamma_{10,0}$(Te)	894,8 (2)	0,00101 (7)
$\gamma_{13,1}$(Te)	909,12 (12)	0,00141 (8)
$\gamma_{12,0}$(Te)	1036,63 (17)	0,00097 (7)
$\gamma_{13,0}$(Tc)	1068,12 (15)	0,00142 (7)

6 Main Production Modes

$\left\{ \begin{array}{l} \mathrm{Sb-121}(\alpha,2\mathrm{n})\mathrm{I-123} \\ \text{Possible impurities : } \mathrm{I-121,\ I-124,\ I-125,\ I-126} \end{array} \right.$

$\mathrm{I-127(p,5n)Xe-123}$

$\left\{ \begin{array}{l} \mathrm{Te-124(p,2n)I-123} \\ \text{Possible impurities : } \mathrm{I-124,\ I-126,\ I-125} \end{array} \right.$

$\left\{ \begin{array}{l} \mathrm{Te-123(p,n)I-123} \\ \text{Possible impurities : } \mathrm{I-124,\ I-126,\ I-130,\ I-125} \end{array} \right.$

$\left\{ \begin{array}{l} \mathrm{Te-122}(\alpha,3\mathrm{n})\mathrm{Xe-123} \\ \text{Possible impurities : } \mathrm{I-125} \end{array} \right.$

$\left\{ \begin{array}{l} \mathrm{Te-123(He-3,3n)Xe-123} \\ \text{Possible impurities : } \mathrm{I-125} \end{array} \right.$

$\left\{ \begin{array}{l} \mathrm{Te-124(He-3,4n)Xe-123} \\ \text{Possible impurities : } \mathrm{I-125} \end{array} \right.$

$\left\{ \begin{array}{l} \mathrm{Te-122(d,n)I-123} \\ \text{Possible impurities : } \mathrm{I-124,\ I-126,\ I-131,\ I-125} \end{array} \right.$

Alpha Decay

Alpha Emission

- An alpha particle is a highly energetic helium nucleus consisting of two neutrons and 2 protons.
- It is normally emitted from isotopes when the neutron-to-proton ratio is too low – through the so-called alpha decay.
- Atomic number and atomic mass number are conserved in alpha decays

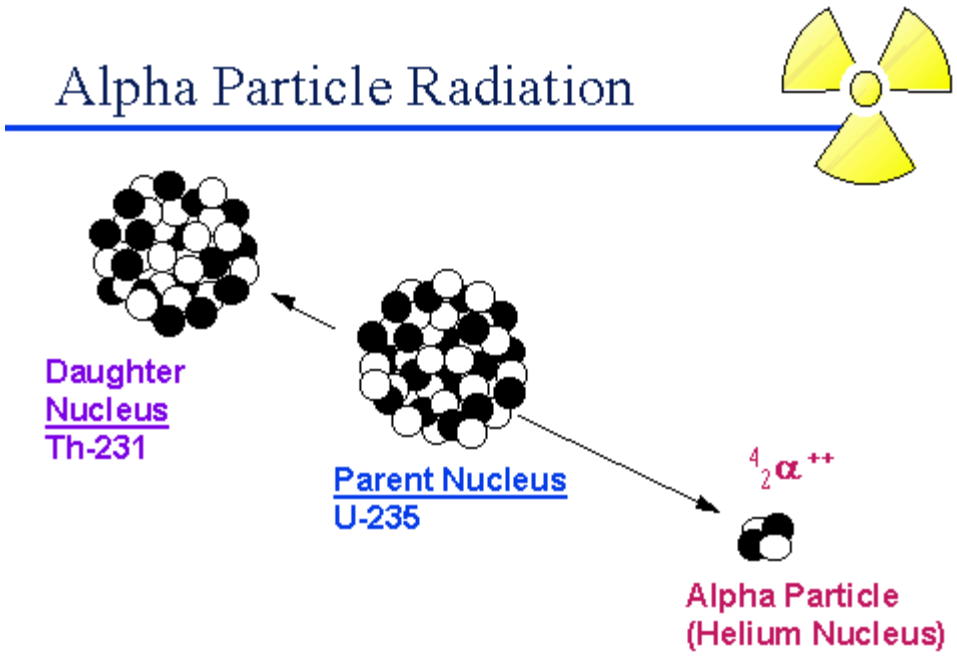

Alpha Emission

- In heavy elements, a potential barrier of ~25MeV has to be overcome for an alpha particle to escape from the potential well.
- It would require a minimum kinetic energy of ~3.8MeV for the alpha particle to "tunneling through" the potential well is

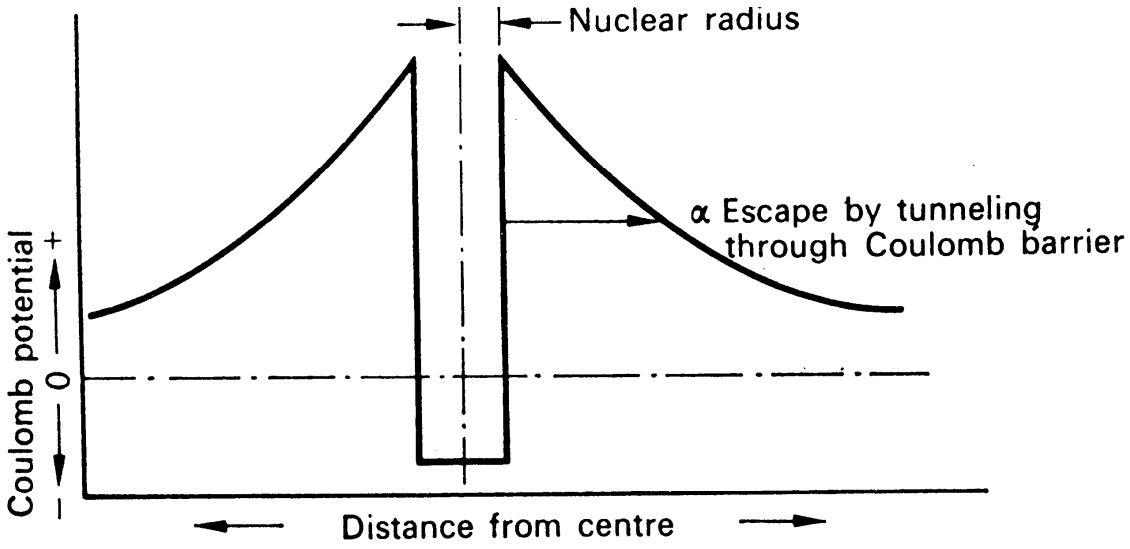

FIG. 4.1. Potential inside and in the vicinity of a nucleus.

Energy Spectra of Alpha Particles

Alpha decays are sometimes accompanied by the excited daughter products which complicates the resultant alpha particle spectra.

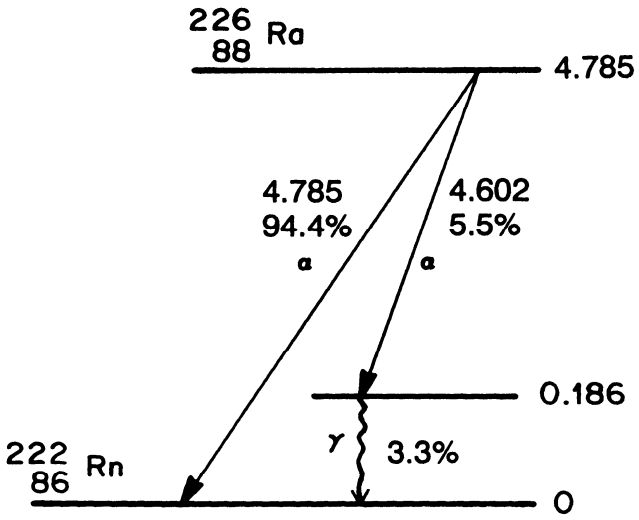

FIGURE 3.4. Nuclear decay scheme of $^{226}_{88}Ra$.

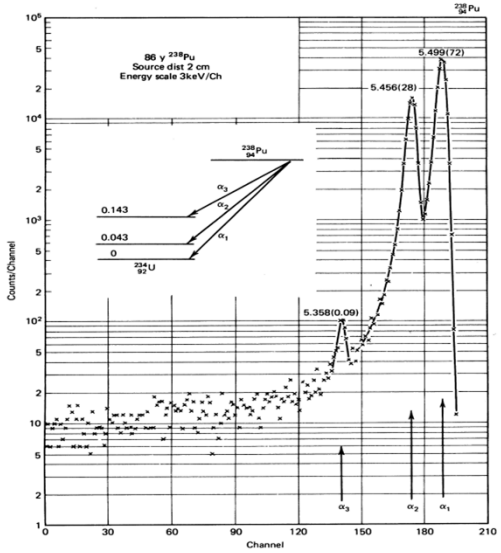

Measured energy spectrum of alpha particles emitted from the decay of ^{238}Pu.

The kinetic energy of alpha particles generated is given by

$$E_\alpha = Q \cdot (A-4)/A$$

Energy Release in Alpha Emission

- The required kinetic energy has to come from the decrease in mass following the decay process.
- The relationship between mass and energy associated with an alpha emission is given as

$$M_p = M_d + M_\alpha + 2M_e + Q, \tag{4.1}$$

where M_p, M_d, M_α, and M_e are respectively equal to the masses of the parent, the daughter, the emitted alpha particle, and the two orbital electrons that are lost during the transition to the lower atomic numbered daughter, while Q is the total energy release associated with the radioactive transformation.

Energy Loss Mechanisms

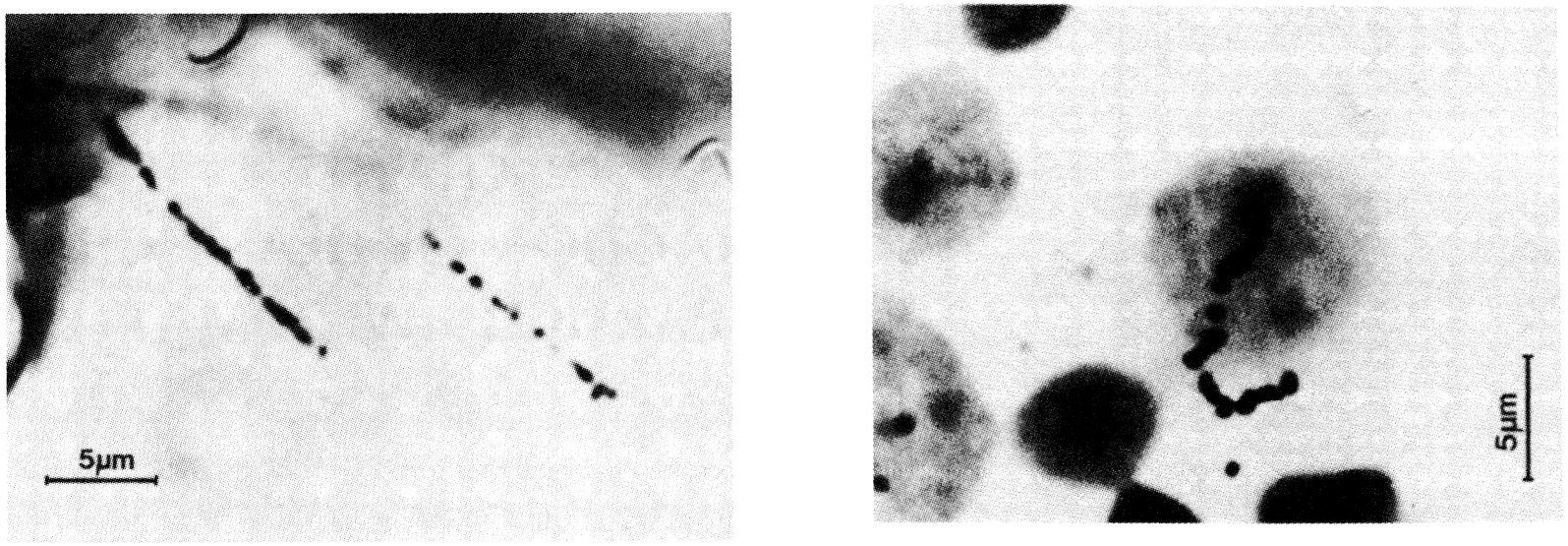

FIGURE 5.1. (Top) Alpha-particle autoradiograph of rat bone after inhalation of ^{241}Am. Biological preparation by R. Masse and N. Parmentier. (Bottom) Beta-particle autoradiograph of isolated rat-brain nucleus. The ^{14}C-thymidine incorporated in the nucleolus is located at the track origin of the electron emitted by the tracer element. Biological preparation by M. Wintzerith and P. Mandel. (Courtesy R. Rechenmann and E. Wittendorp-Rechenmann, Laboratoire de Biophysique des Rayonnements et de Methodologie INSERM U.220, Strasbourg, France.)

Single Collision Energy-Loss Spectrum

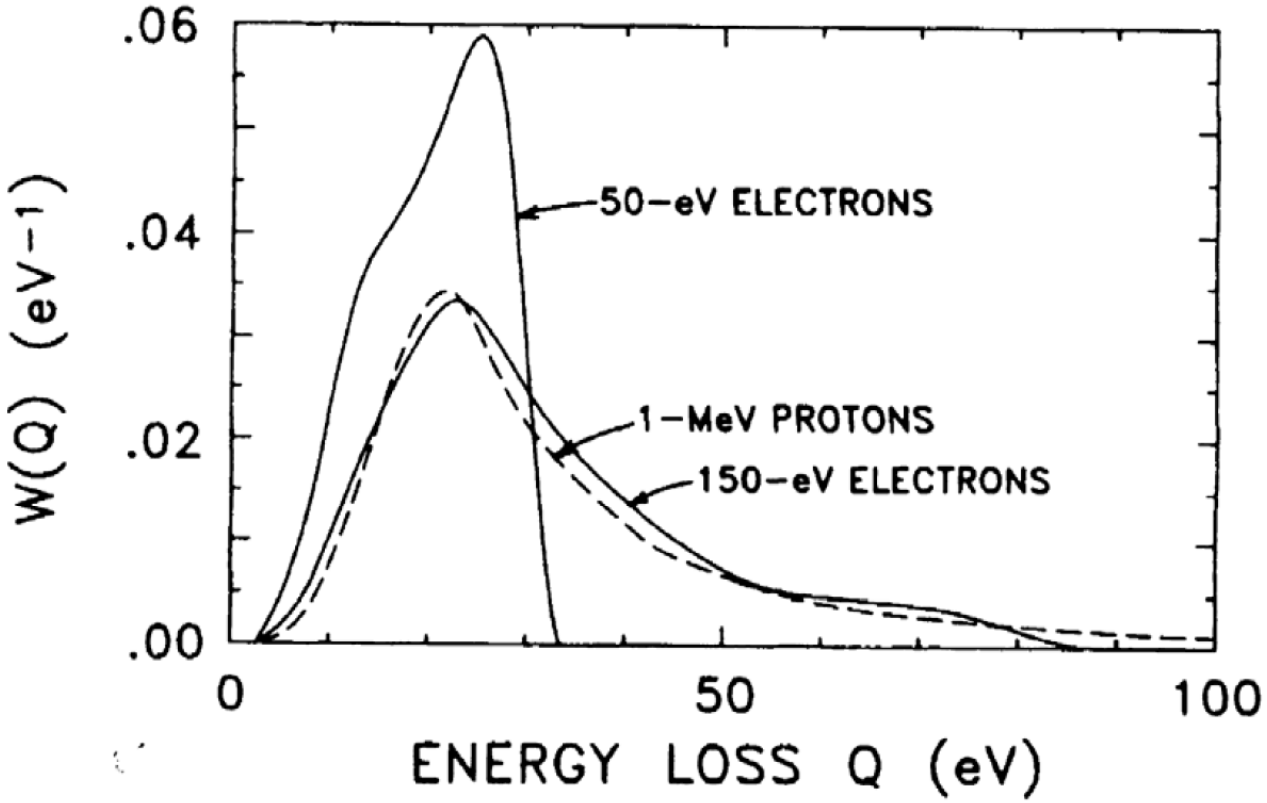

Fig. 5.3 Single-collision energy-loss spectra for 50-eV and 150-eV electrons and 1-MeV protons in liquid water. (Courtesy Oak Ridge National Laboratory, operated by Martin Marietta Energy Systems, Inc., for the Department of Energy.)

Targeted Therapy – Basic Principles

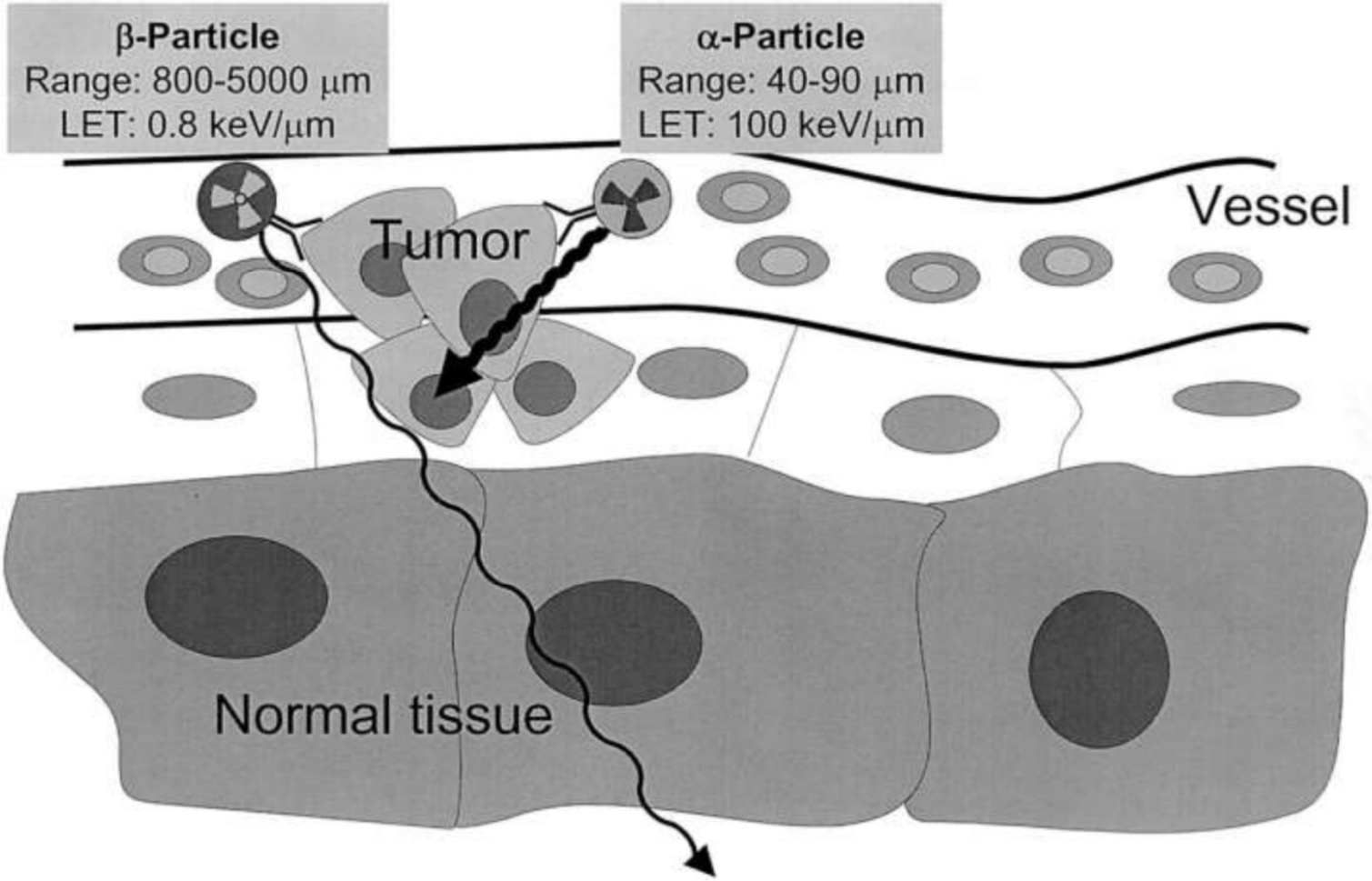

http://www.icrp.org/docs/icrp2017/18%20Lassman%20Presentation.pdf

Alpha emitting isotopes for therapeutic applications in nuclear medicine

Radionuclide	Half-Life	Max. Particle Energy
At-211	7.2 hrs	6.0 MeV
Bi-213	46 min	6.0 MeV
Ra-223	11.4 days	5.8 MeV
Ac-225	10.0 days	5.9 MeV

http://www.icrp.org/docs/icrp2017/18%20Lassman%20Presentation.pdf

Decay of Ra-223

Decay Chain	Branching Ratio	Half-life	Alpha and Recoil Nuclei (MeV)	Beta and Auger Electrons (MeV)	Gamma and X-Rays (MeV)
Ra-223		11.43 days	5.77	0.078	0.141
Rn-219	100%	3.96 s	6.88	0.007	0.059
Po-215	100%	1.78 ms	7.49	0.000	0.000
Pb-211	100%	36.10 min	-	0.454	0.064
Bi-211	100%	2.14 min	6.66	0.010	0.047
Tl-207	99.7%	4.77 min	-	0.494	0.002
Po-211	0.3%	0.52 s	7.61	0.000	0.008

http://www.icrp.org/docs/icrp2017/18%20Lassman%20Presentation.pdf

Biodistribution of Ra-223

Original article

Nuclear Medicine Communications

Quantitative imaging of ^{223}Ra-chloride (Alpharadin) for targeted alpha-emitting radionuclide therapy of bone metastases

Cecilia Hindorf[a,d], Sarah Chittenden[a], Anne-Kirsti Aksnes[c], Chris Parker[b] and Glenn D. Flux[a]

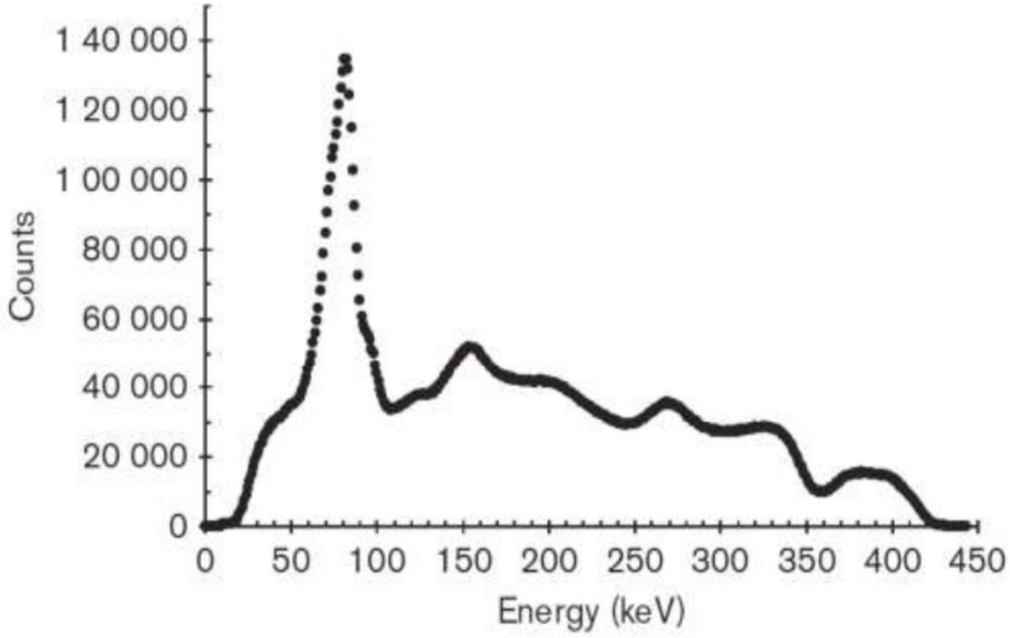

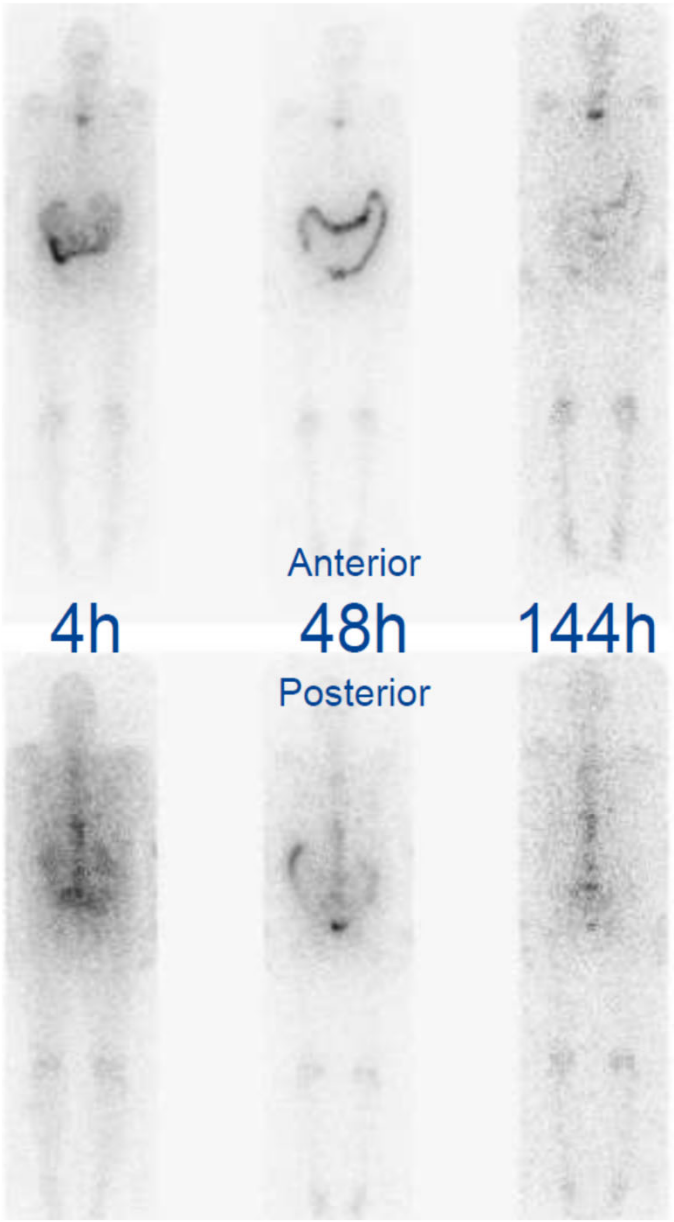

European Journal of Nuclear Medicine and Molecular Imaging
January 2016, Volume 43, Issue 1, pp 21–33 | Cite as

Dosimetry of bone metastases in targeted radionuclide therapy with alpha-emitting ^{223}Ra-dichloride

Authors | Authors and affiliations

Massimiliano Pacilio, Guido Ventroni, Giuseppe De Vincentis, Bartolomeo Cassano, Rosanna Pellegrini, Elisabetta Di Castro, Viviana Frantellizzi, Giulia Anna Follacchio, Tatiana Garkavaya, Leda Lorenzon, Pasquale Ialongo, Roberto Pani, Lucio Mango

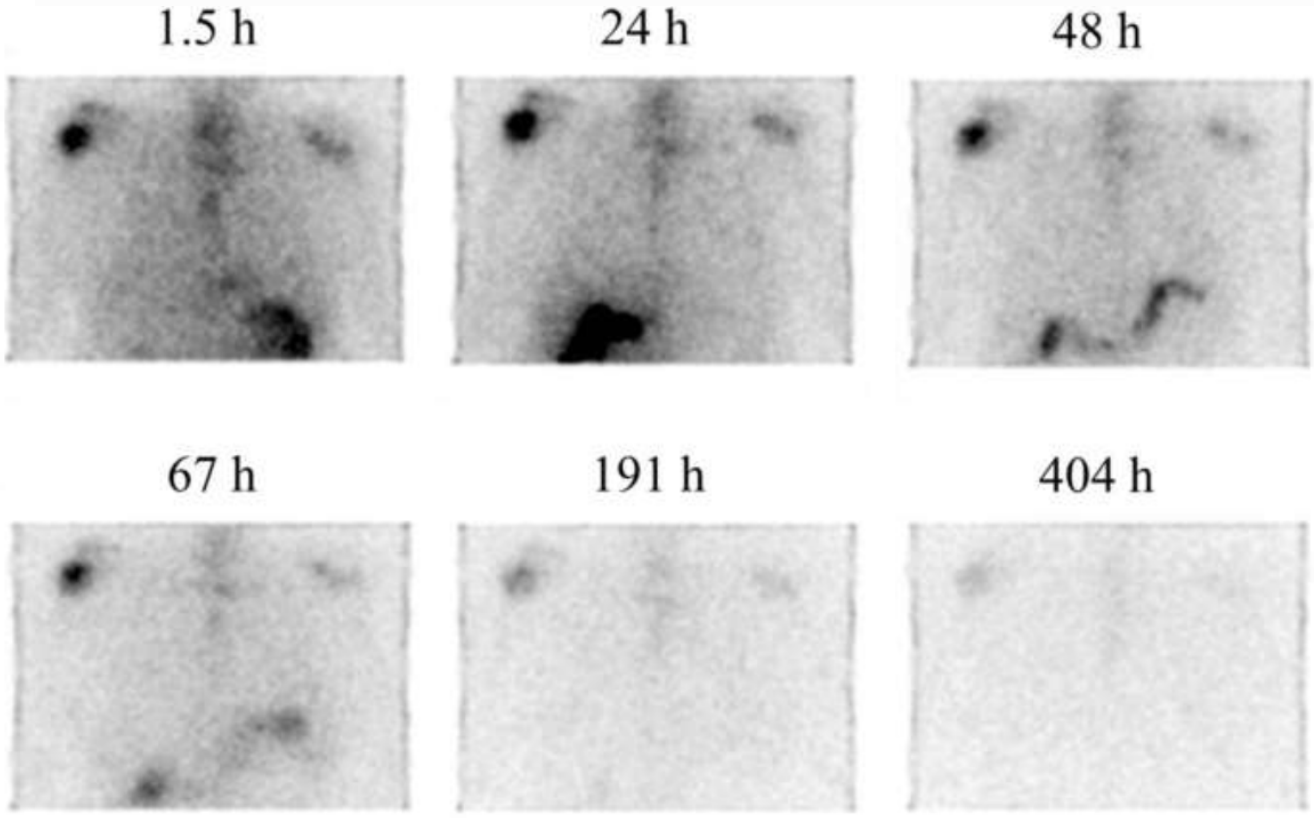

http://www.icrp.org/docs/icrp2017/18%20Lassman%20Presentation.pdf

Therapeutic Radiometals Beyond ^{177}Lu and ^{90}Y: Production and Application of Promising α-Particle, β$^-$-Particle, and Auger Electron Emitters

Cristina Müller[1,2], Nicholas P. van der Meulen[1,3], Martina Benešová[1,2], and Roger Schibli[1,2]

[1]Center for Radiopharmaceutical Sciences ETH-PSI-USZ, Paul Scherrer Institut, Villigen-PSA, Switzerland; [2]Department of Chemistry and Applied Biosciences, ETH Zurich, Zurich, Switzerland; and [3]Laboratory of Radiochemistry, Paul Scherrer Institut, Villigen-PSA, Switzerland

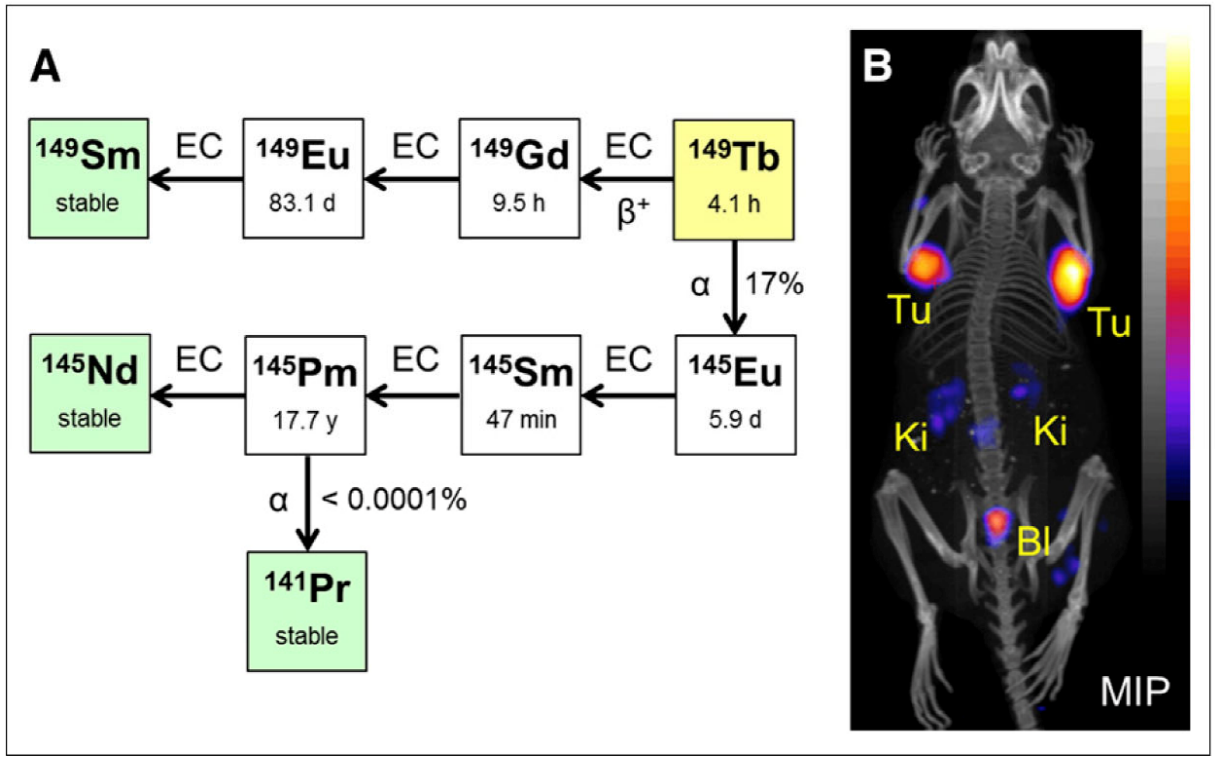

FIGURE 1. (A) Decay of ^{149}Tb to stable ^{149}Sm, ^{145}Nd, and ^{141}Pr. EC = electron capture. (B) Maximum-intensity projection (MIP) of PET/CT image of AR42J tumor–bearing mouse 2 h after injection of ^{149}Tb-DOTANOC (7 MBq). Bl = urinary bladder; Ki = kidney; Tu = tumor. (Adapted with permission of (*45*).)

TERBIUM-149

^{149}Tb was first proposed for targeted α-therapy by Allen and Blagojevic (*41*). Unlike most α-emitters, it decays predominantly by the emission of a single low-energy α-particle, positrons, and γ-radiation (Fig. 1A) (*42*). Beyer et al. chose the Nd(^{12}C,5n)^{149}Dy→^{149}Tb production route at the European Organization for Nuclear Research (*42*). Later, ^{149}Tb was produced by proton-induced spallation of a tantalum target followed by an online isotope separation process (*37,42,43*). In this scenario, ^{149}Tb had to be separated from isobars and pseudoisobars with a mass of 149 using cation-exchange chromatography (*37,42,43*).

The first preclinical therapy study with ^{149}Tb was performed in a mouse model of leukemia with ^{49}Tb-labeled cyclohexane-DTPA–functionalized rituximab (*43*). This therapy resulted in the long-term survival of mice without evidence of recurrence 120 d after

Therapeutic Radiometals Beyond ^{177}Lu and ^{90}Y: Production and Application of Promising α-Particle, β$^-$-Particle, and Auger Electron Emitters

Cristina Müller[1,2], Nicholas P. van der Meulen[1,3], Martina Benešová[1,2], and Roger Schibli[1,2]

[1]Center for Radiopharmaceutical Sciences ETH-PSI-USZ, Paul Scherrer Institut, Villigen-PSA, Switzerland; [2]Department of Chemistry and Applied Biosciences, ETH Zurich, Zurich, Switzerland; and [3]Laboratory of Radiochemistry, Paul Scherrer Institut, Villigen-PSA, Switzerland

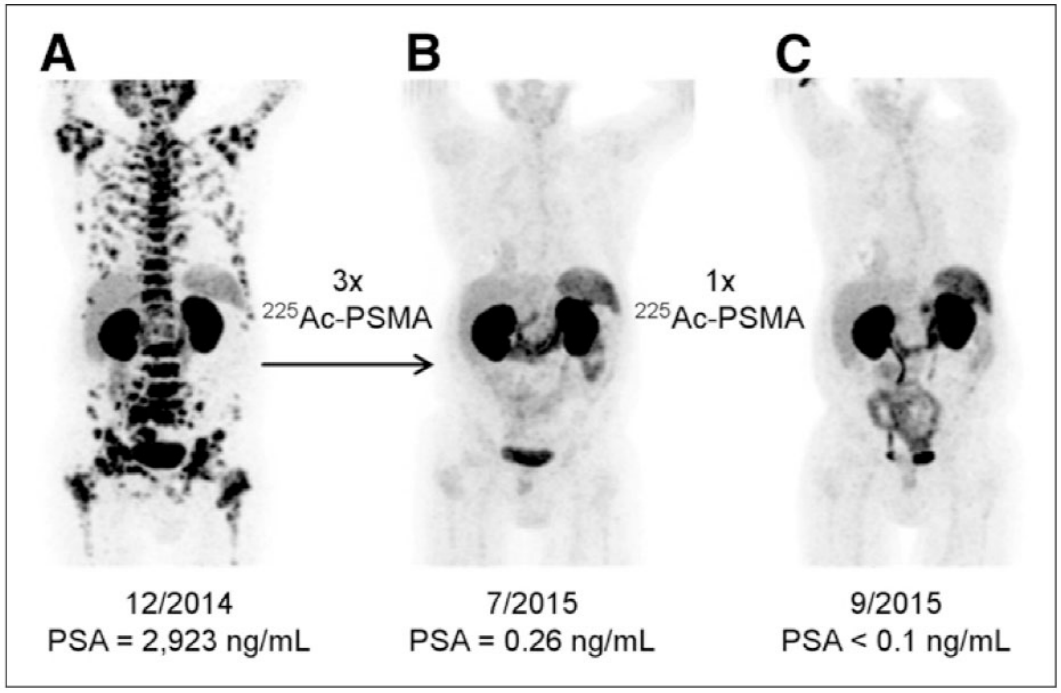

FIGURE 4. (A) ^{68}Ga-PSMA-11 PET/CT scan of patient with prethera-peutic tumor spread. PSA = prostate-specific antigen. (B) Restaging 2 mo after third cycle of ^{225}Ac-PSMA-617 (9–10 MBq). (C) Restaging 2 mo after single additional consolidation therapy (6 MBq). ^{177}Lu-PSMA-617 was contraindicated because of diffuse red marrow infiltration. (Reproduced from (*68*).)

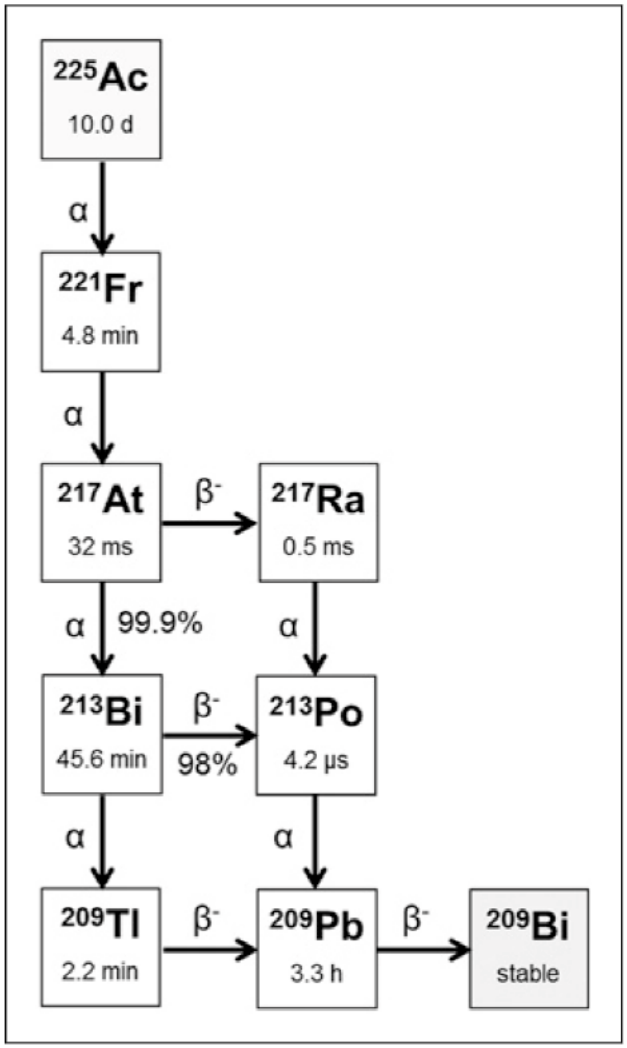

FIGURE 3. Decay of ^{225}Ac to ^{213}Bi and stable ^{209}Bi.

X-Rays Sources

What Can We Learn from X-rays?

"The radiograph of Bera Rontgen's hand", taken 22 Dec. 1895

Wilhelm Conrad Röntgen,
The Nobel Prize in Physics 1901.

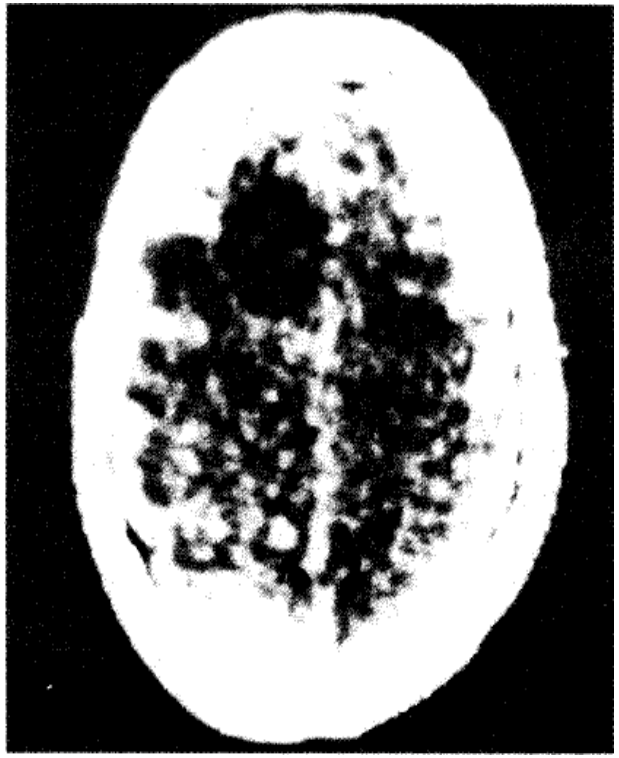

A brain image from the first prototype clinical CT imager, 1972.

Godfrey N. Hounsfield, The Nobel Prize in Physiology or Medicine 1979

X-ray Imaging Examples

Double mandibular fracture with strong displacement to the left.

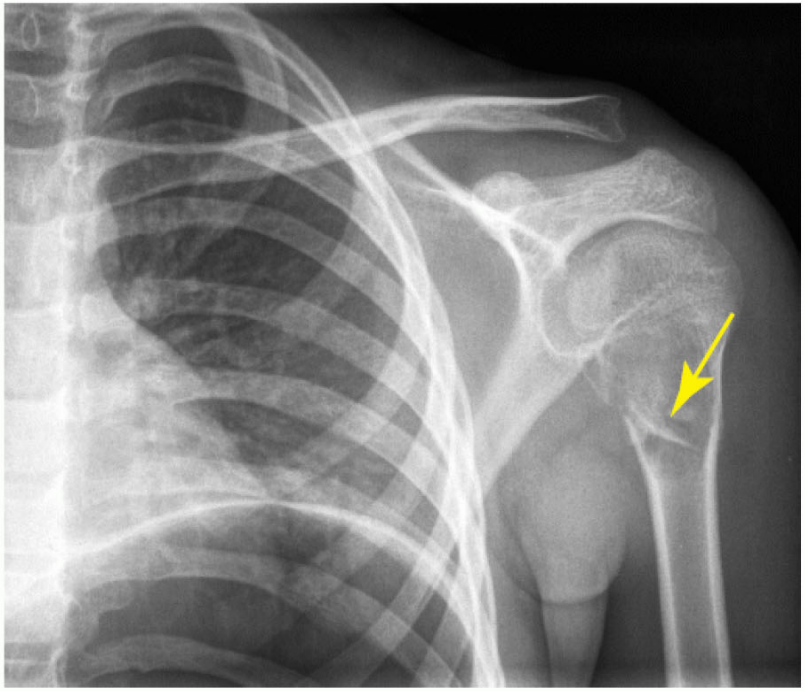

Solitary humeral bone cyst known as ”fallen leaf sign”

Covered in lecture

Sources of Electromagnetic Radiation – X-ray Emission Through Bremsstrahlung

- When fast electrons decelerated in the Coulomb field of a nucleus, part of its energy is converted into electromagnetic radiation in the form of Bremsstrahlung (a Germen word for “braking radiation”).

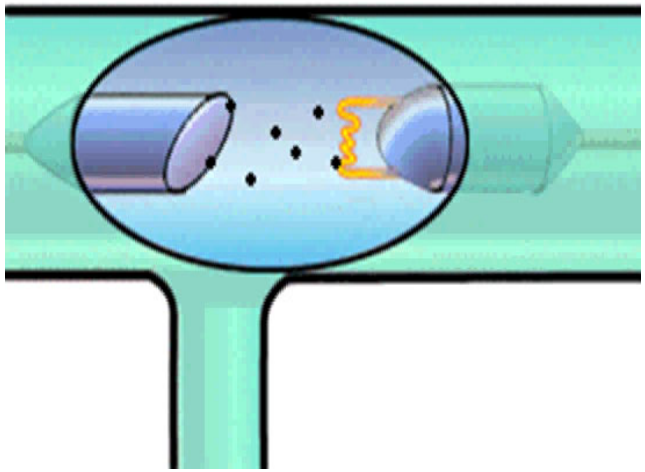

Covered in lecture

X-ray Generation – Bremmstrahlung

- Target nucleus positive charge ($Z \cdot p^+$) attracts incident e^-
- Deceleration of an incident e^- occurs in the proximity of the target atom nucleus
- E lost by e^- is gained by the EM photon (x-ray) generated
  - The impact parameter distance, the closest approach to the nucleus by the e^- determines the amount of E loss
  - The Coulomb force of attraction varies strongly with distance ($\propto 1/r^2$); ↓ distance → ↑ deceleration and E loss → ↑ photon E
  - Direct impact on the nucleus determines the maximum x-ray E (E_{max})

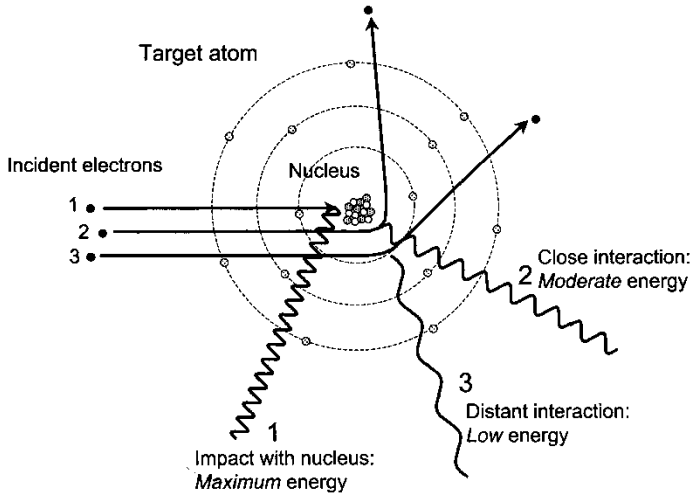

Covered in lecture

Bremmstrahlung X-ray Energy Spectrum

Interestingly, this process creates a relatively uniform spectrum.

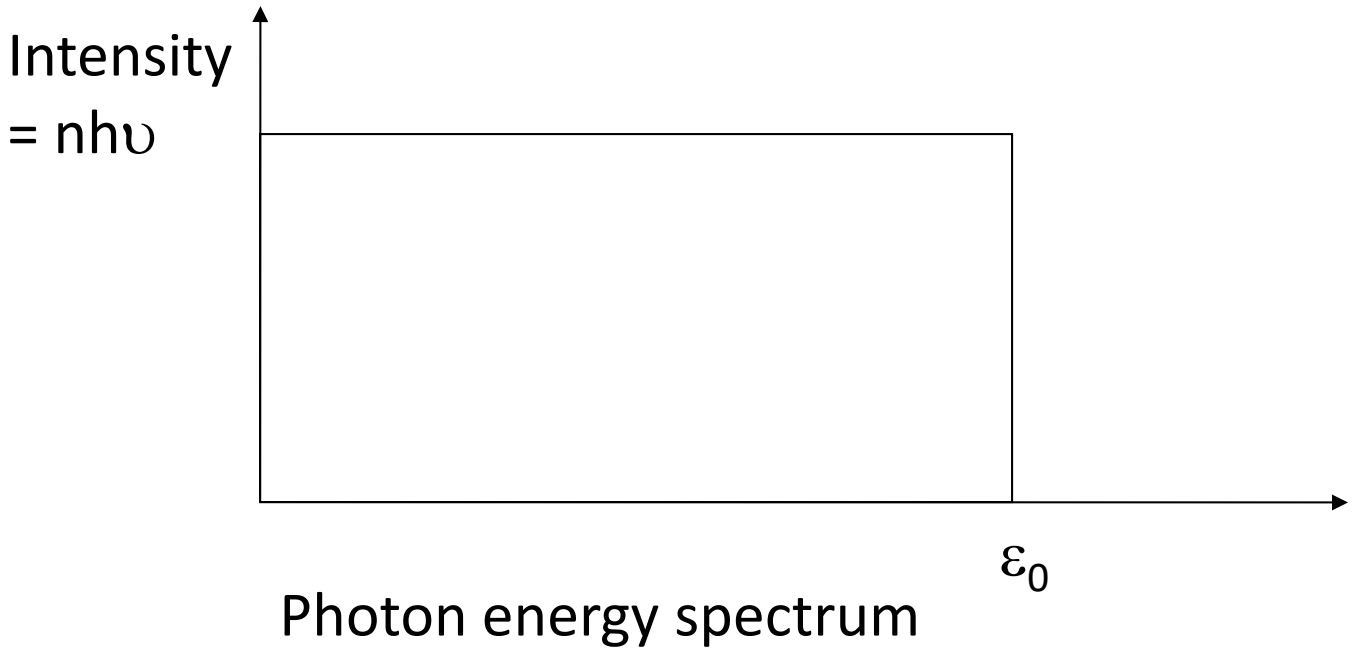

Covered in lecture

The Unfiltered Bremsstrahlung Spectrum
Thick Target X-ray Formation

We can model target as a series of thin targets. Electrons successively loses energy as they moves deeper into the target.

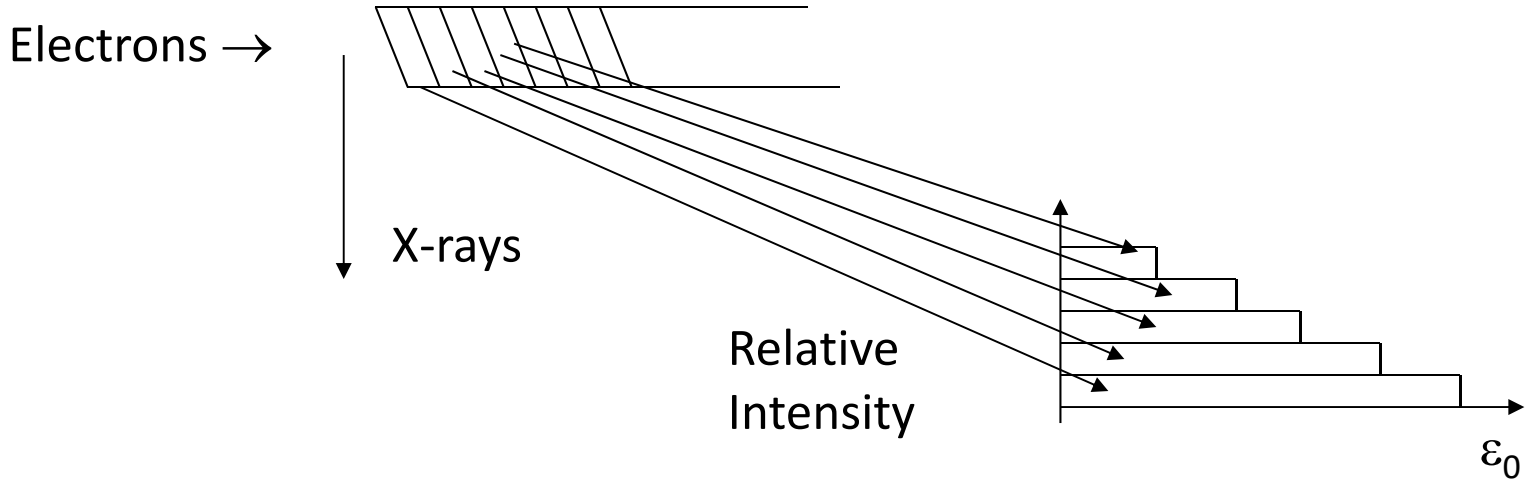

Each layer produces a flat energy spectrum with decreasing peak energy level.

Covered in lecture

X-ray Generation – Characteristic X-rays

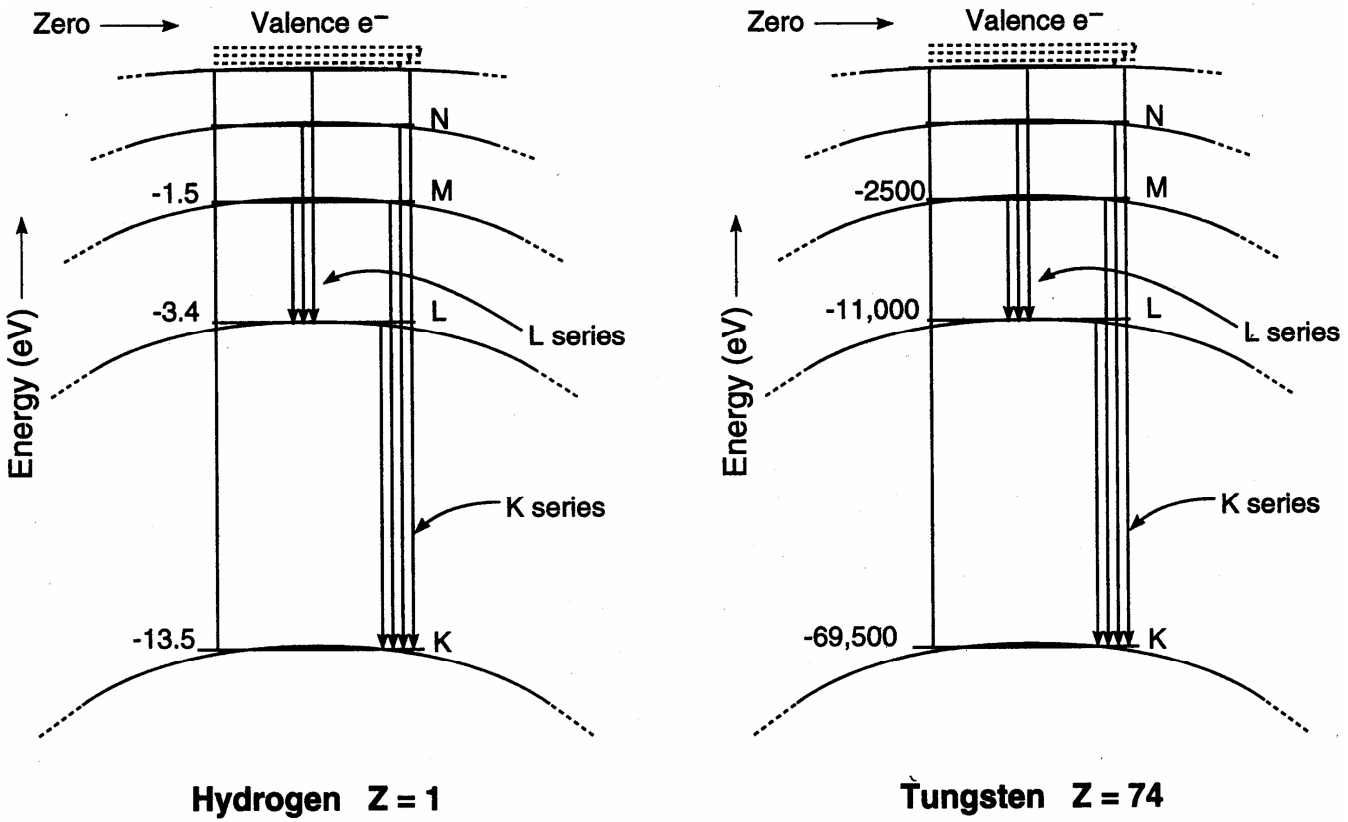

Electron binding energy

Covered in lecture

X-ray Generation – Characteristic X-rays

- e^- of the target atom have a binding energy (BE)that depends on atomic Z (rem: $BE_K \propto Z^2$) and the shell ($BE_K > BE_L > BE_M > \ldots$)
- When e^-(KE) incident on the target exceeds the target atom e^-(BE), it's energetically possible for a collisional interaction to eject the bound electron and ionize the atom.
- What would happen then?

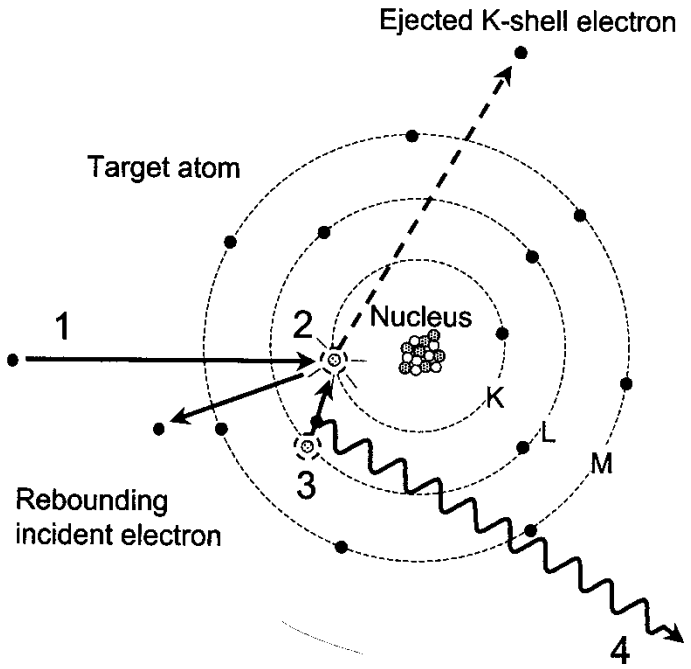

Covered in lecture

X-ray Generation – Characteristic X-rays

- Within each shell (other than K) there are discrete E orbitals (ℓ = 0, 1, ... , n-1) → characteristic x-ray fine E splitting
- Characteristic x-rays other than those generated through K-shell transitions are unimportant

TABLE 5-2. K-SHELL CHARACTERISTIC X-RAY ENERGIES (keV) OF COMMON X-RAY TUBE TARGET MATERIALS[a]

Shell Transition	Tungsten	Molybdenum	Rhodium
$K_{\alpha 1}$	59.32	17.48	20.22
$K_{\alpha 2}$	57.98	17.37	20.07
$K_{\beta 1}$	67.24	19.61	22.72

[a]*Note:* Only prominent transitions are listed.

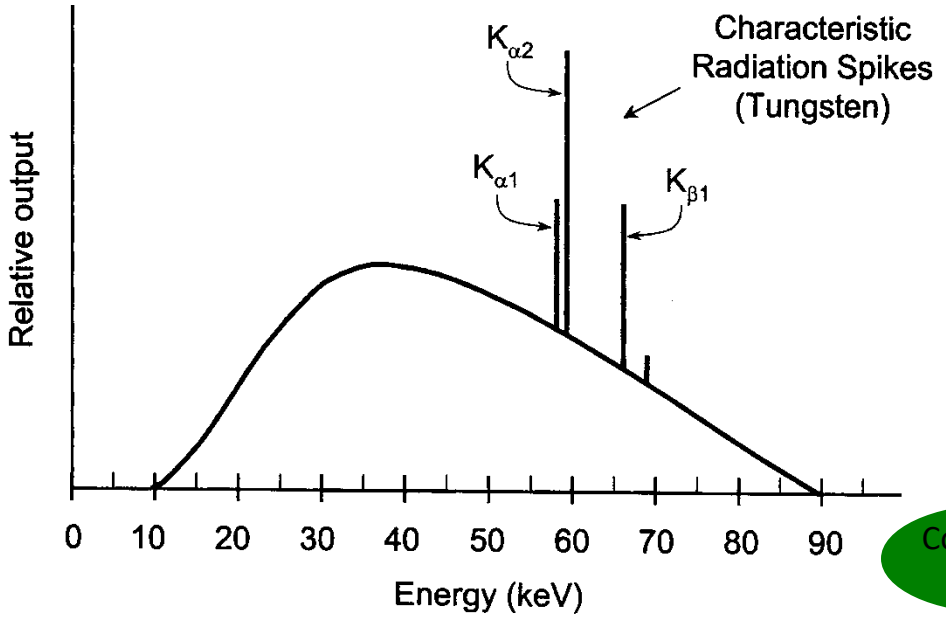

Covered in lecture

Physical Designs Considerations

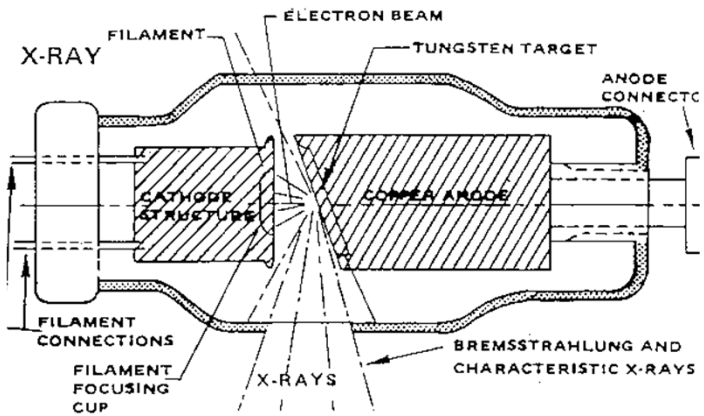

Typical micro-focus X-ray source

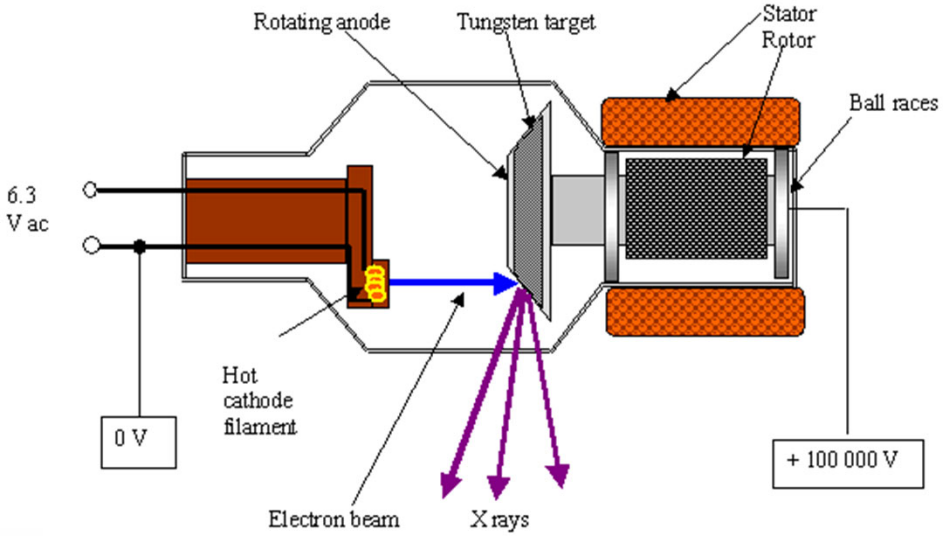

Rotating anode X-ray source

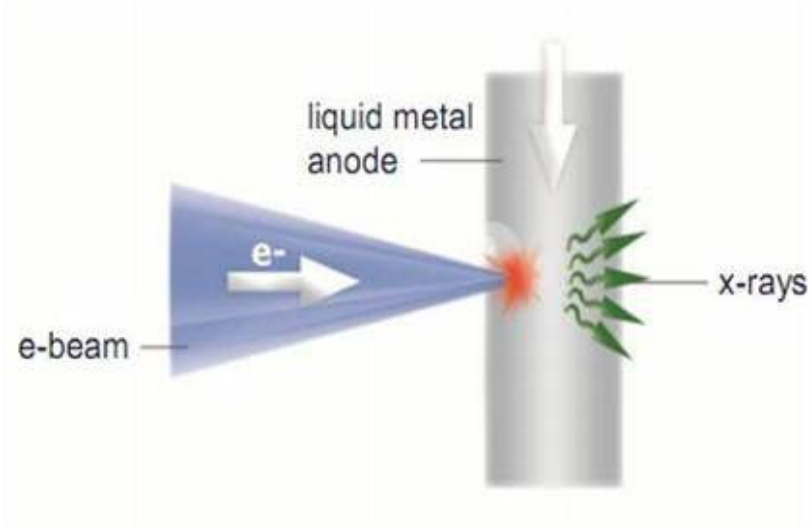

(Left) Liquid metal jet anode
http://www.excillum.com/technology/metal-jet-technology.html

X-ray Generation – X-ray Tube

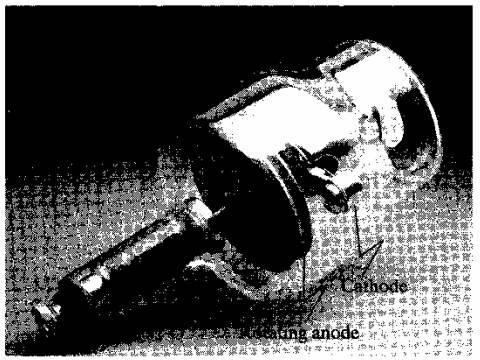

Figure 5.3
An x-ray tube.

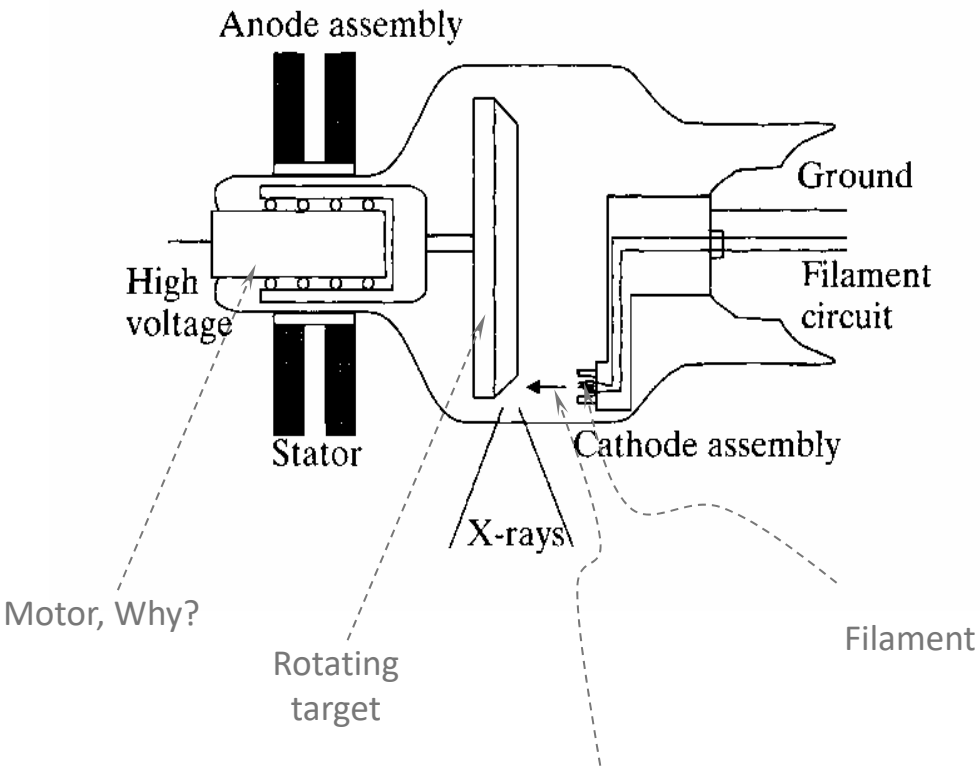

Figure 5.4
Schematic diagram of an x-ray tube.

X-ray Generation – Characteristic X-rays

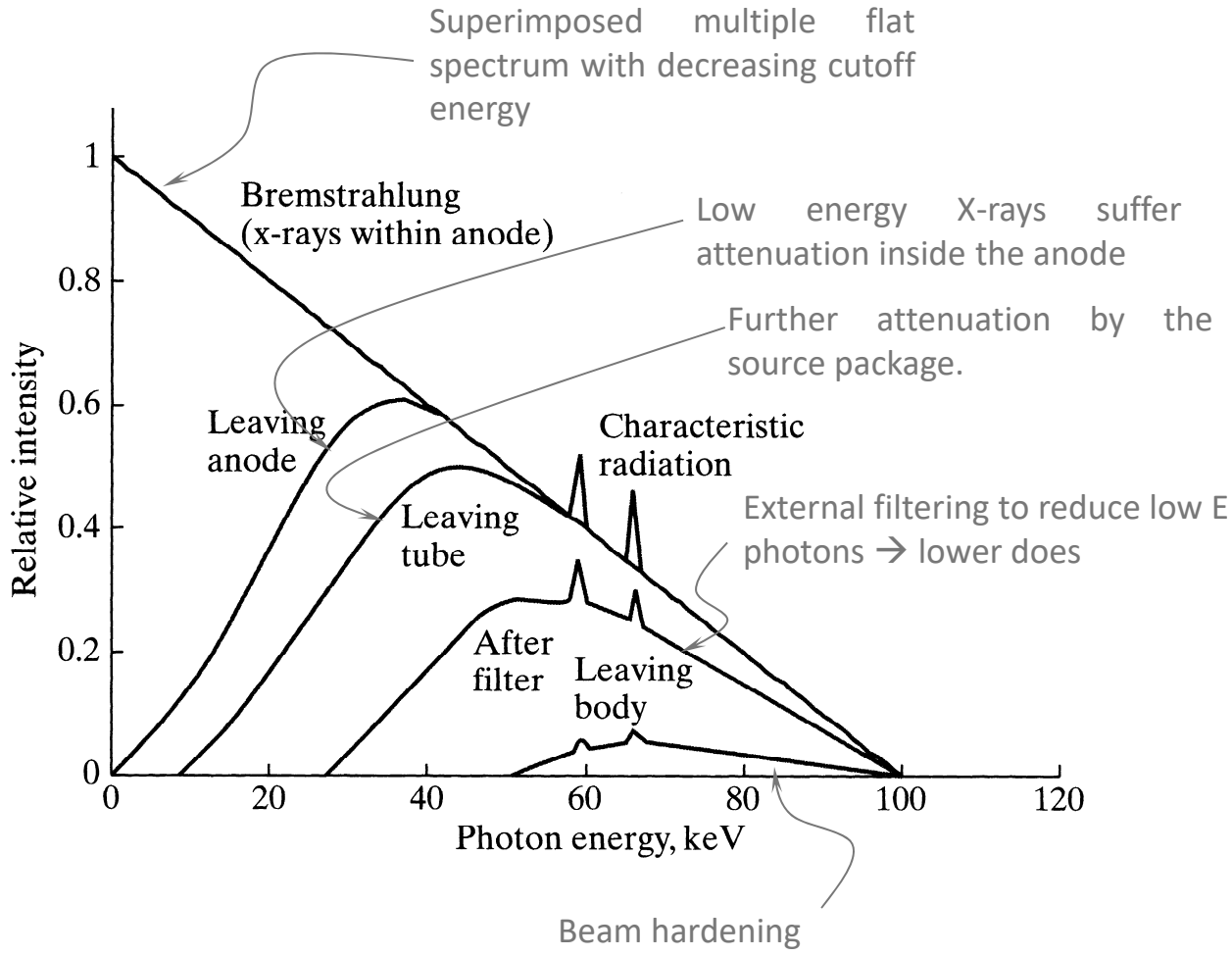

Figure 5.5
Relative intensity of x-ray photons. (Adapted from Webster, 1998. This material is used by permission of John Wiley & Sons, Inc.)

X-ray Computed Tomography (CT)

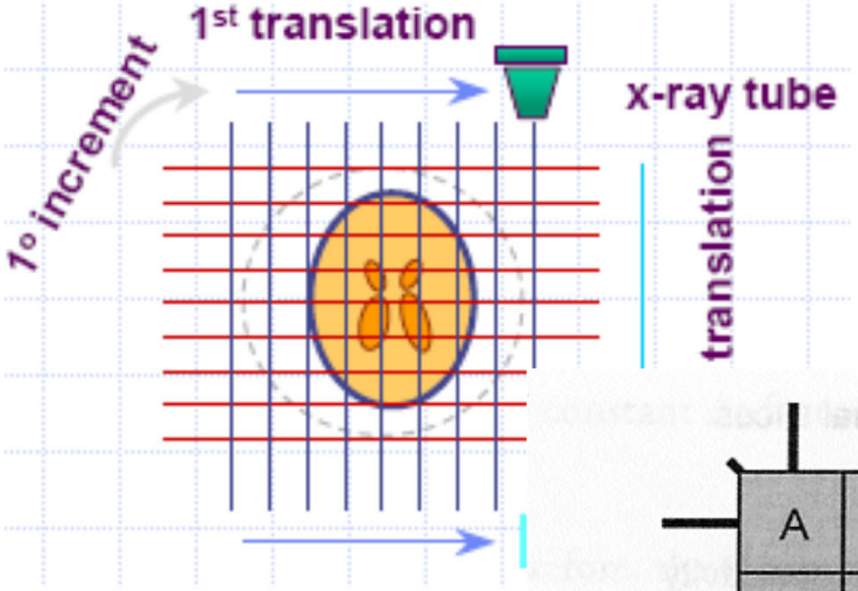

0.2 % attenuation change detectable in CT Images !!

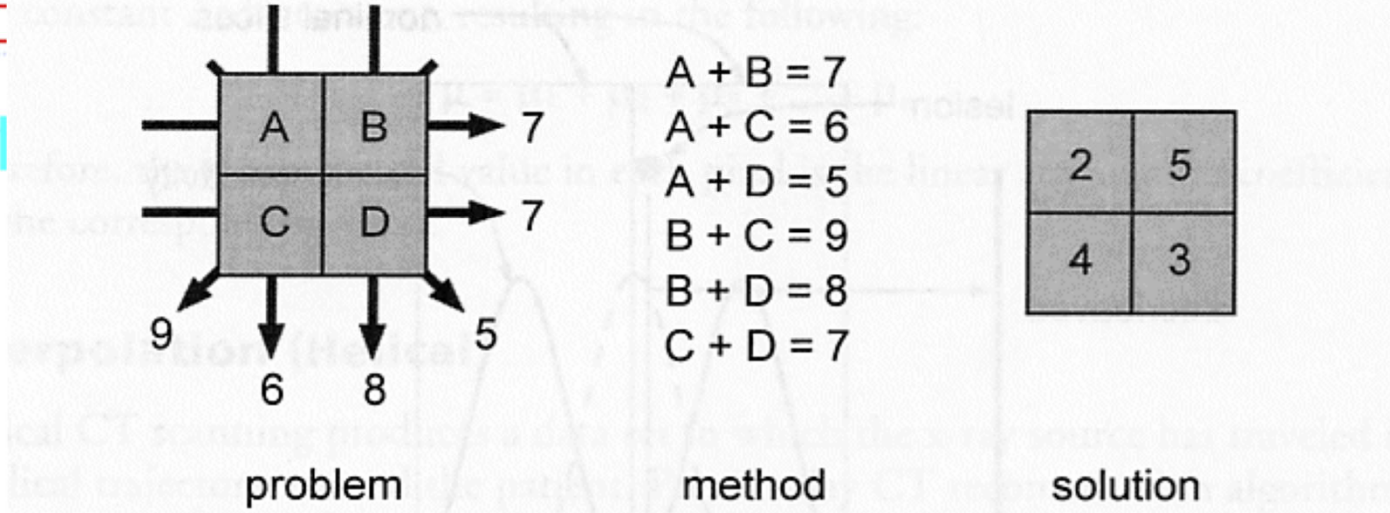

FIGURE 13-27. The mathematical problem posed by computed tomographic (CT) reconstruction is to calculate image data (the pixel values—A, B, C, and D) from the projection values *(arrows)*. For the simple image of four pixels shown here, algebra can be used to solve for the pixel values. With the six equations shown, using substitution of equations, the solution can be determined as illustrated. For the larger images of clinical CT, algebraic solutions become unfeasible, and filtered backprojection methods are used.

Example of Potential Problems Caused by the Imperfection of X-ray Sources – Beam Hardening

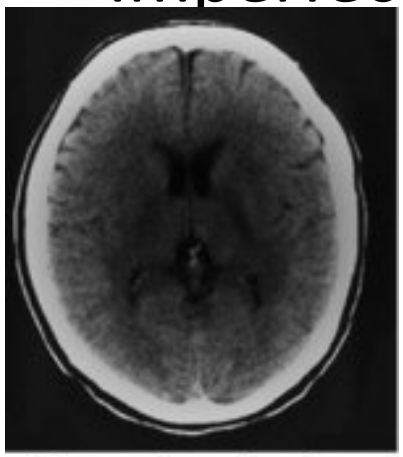

Beam hardening with cupping

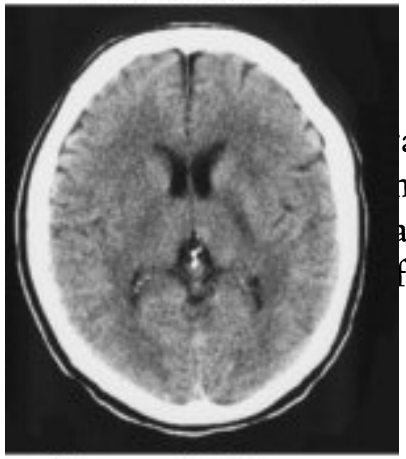

Normal CT scan

ay
n
aterial
f John

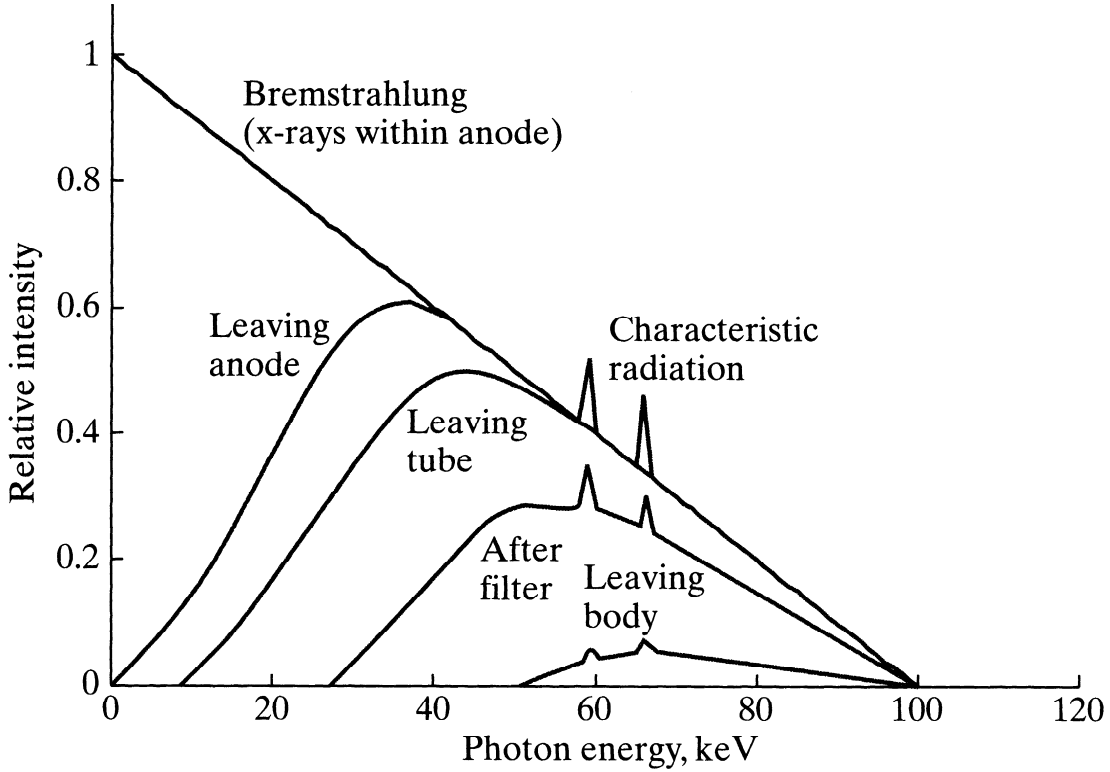

Example of Potential Problems Caused by the Imperfection of X-ray Sources – Beam Hardening

Scout image

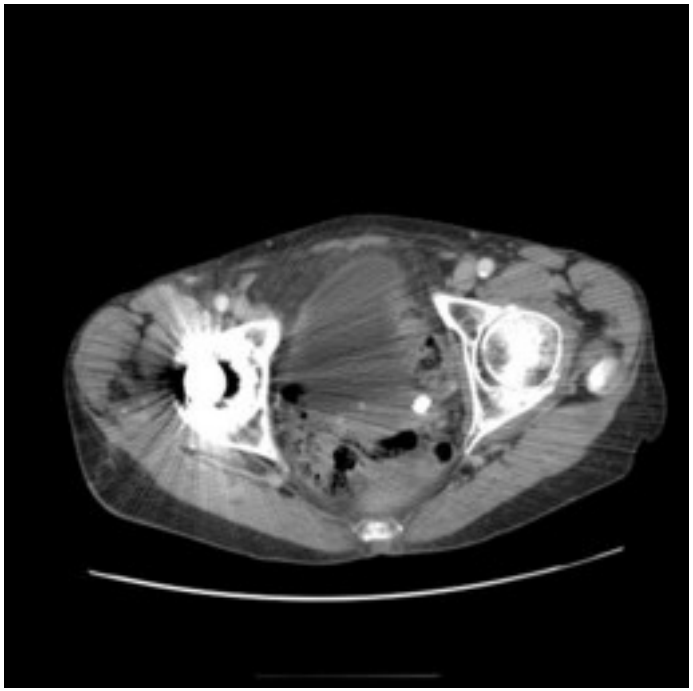

CT images with artifacts due to beam hardening

Beam hardening artifact occurs because the algorithm that reconstructs the image fails when faced with an interface between a high-density structure such as a metallic prosthesis or thick bone and surrounding soft tissue. The 'spray' or 'streak' artifact results. It can be seen in the posterior fossa in most CT brains.

Sources of Electromagnetic Radiation – Bremsstrahlung

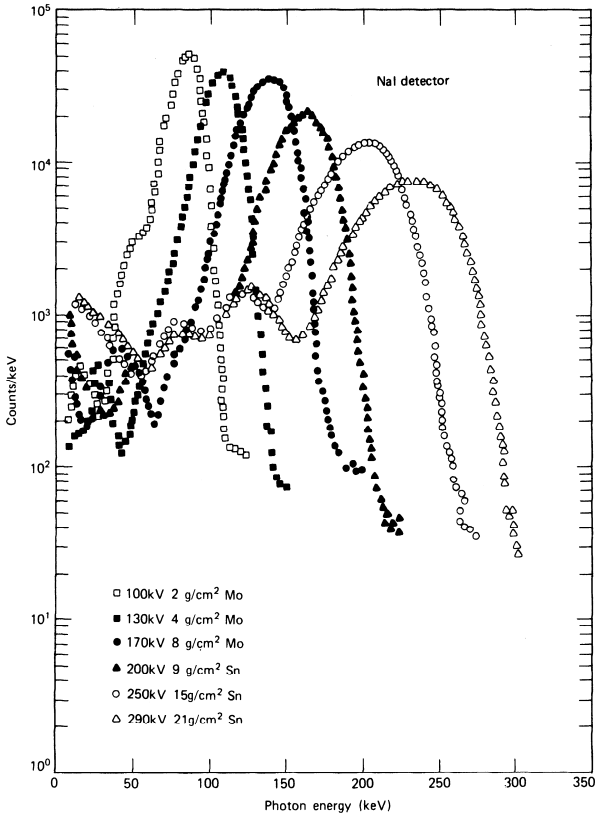

- The bremsstrahlung spectrum can be altered by filtration.
- This is the underlying process for standard X-ray tubes.

Covered in lecture

Synchrotron Radiation

Sources of Electromagnetic Radiation
– Synchrotron Radiation

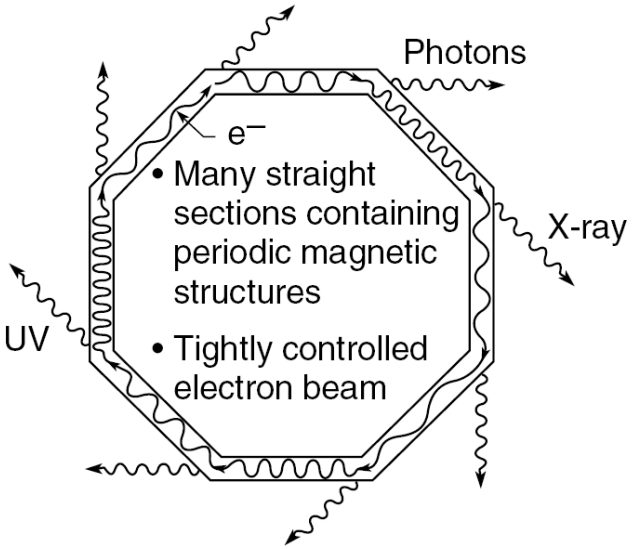

- Emitted when charged particles are accelerated (or decelerated) in a curved path or orbit.
- From visible light (a few eV) to X-ray energies (~10^4eV).
- Very intense !!!

Covered in lecture

Synchrotron Radiation

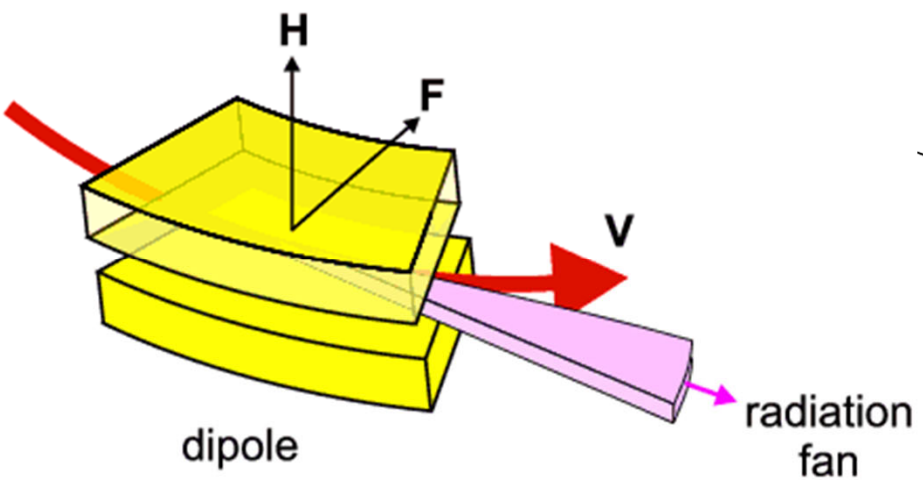

Bending magnet

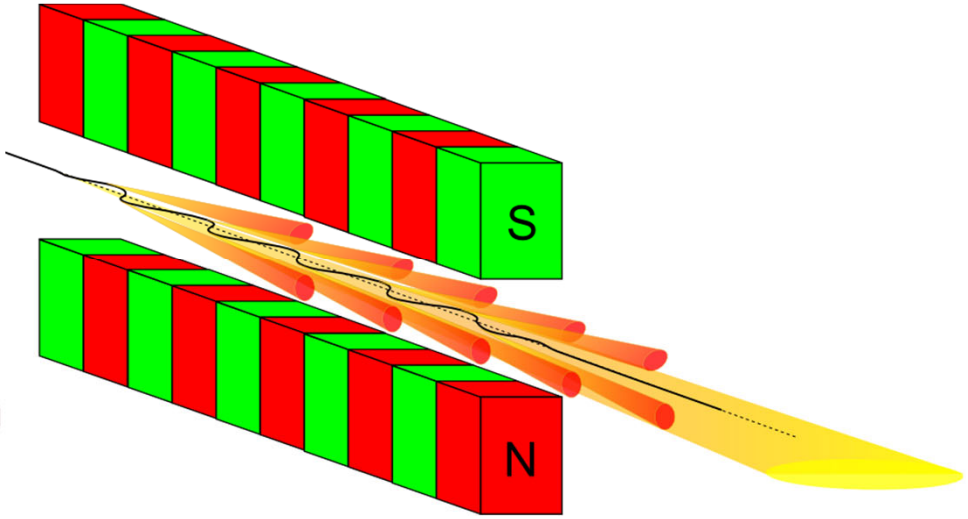

Undulator magnet

https://en.wikipedia.org/wiki/Undulato

Covered in lecture

X-ray Generation – Bremmstrahlung

- Target nucleus positive charge ($Z \cdot p^+$) attracts incident e^-
- Deceleration of an incident e^- occurs in the proximity of the target atom nucleus
- E lost by e^- is gained by the EM photon (x-ray) generated
  - The impact parameter distance, the closest approach to the nucleus by the e^- determines the amount of E loss
  - The Coulomb force of attraction varies strongly with distance ($\propto 1/r^2$); ↓ distance → ↑ deceleration and E loss → ↑ photon E
  - Direct impact on the nucleus determines the maximum x-ray E (E_{max})

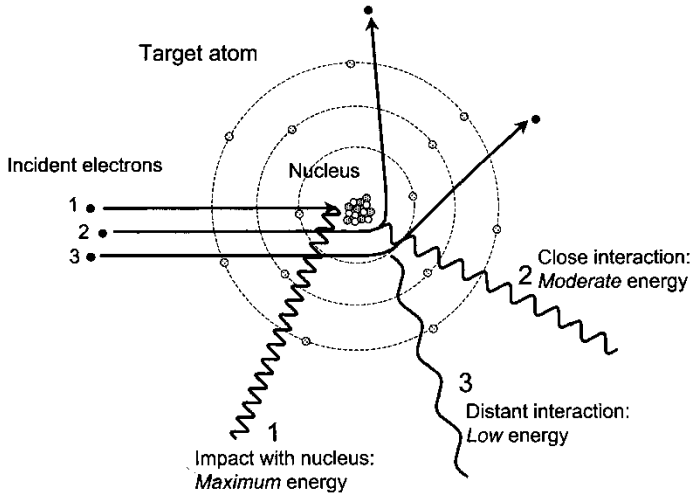

Covered in lecture

Sources of Electromagnetic Radiation
– Selection of X-rays of a Single Energy

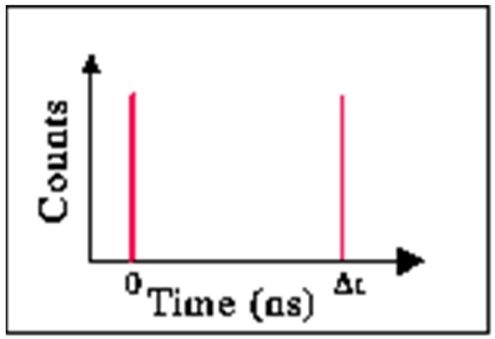

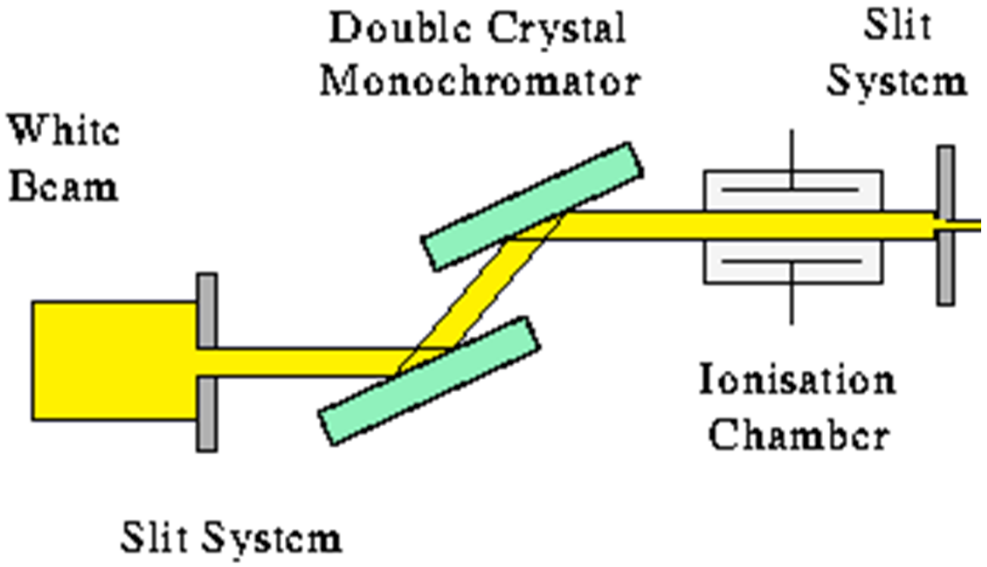

A typical monochromator setup

Covered in lecture

Sources of Electromagnetic Radiation – Synchrotron Radiation

European Synchrotron Radiation Facility

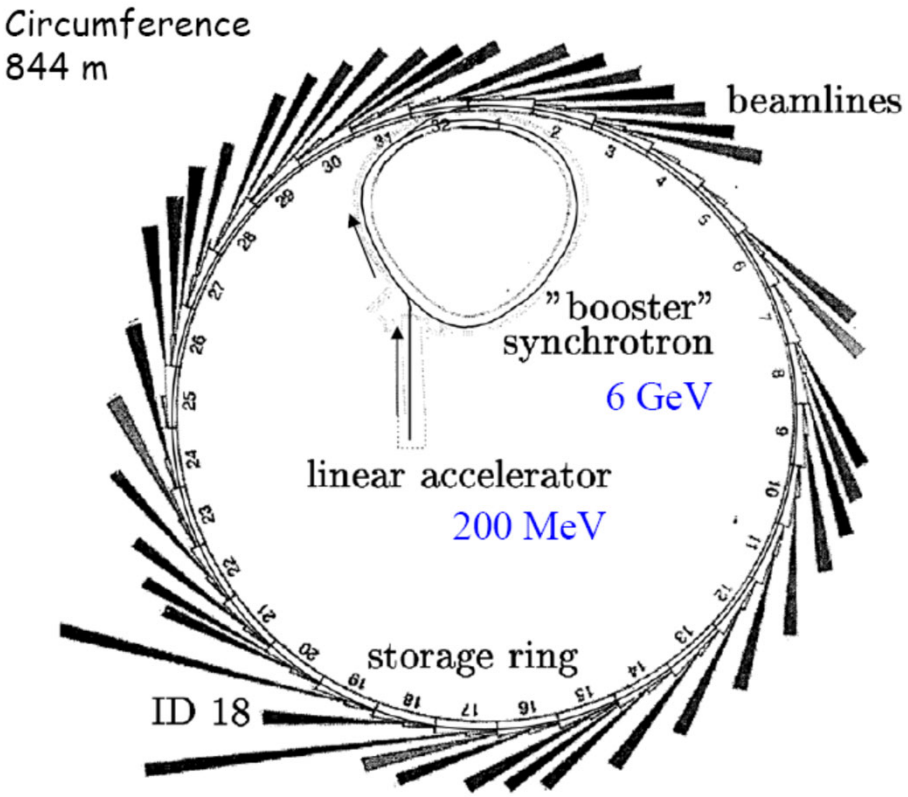

Advanced Photon Source (APS)

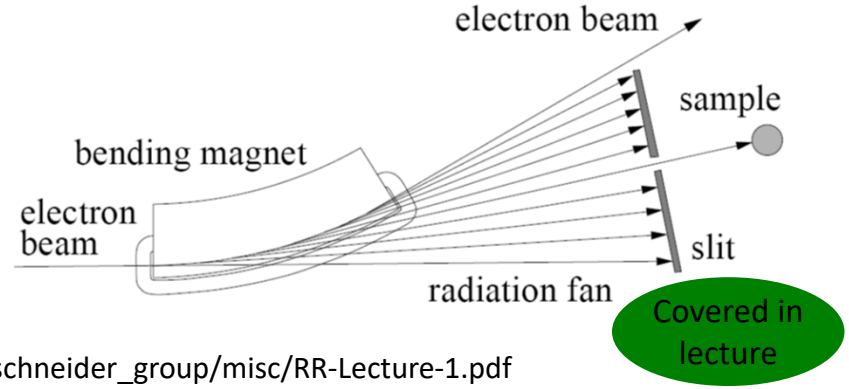

Covered in lecture

From http://www-hasylab.desy.de/science/groups/schneider_group/misc/RR-Lecture-1.pdf

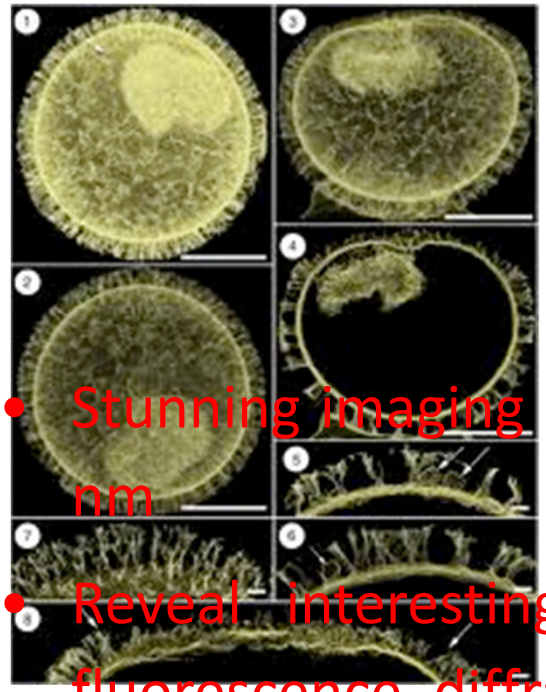

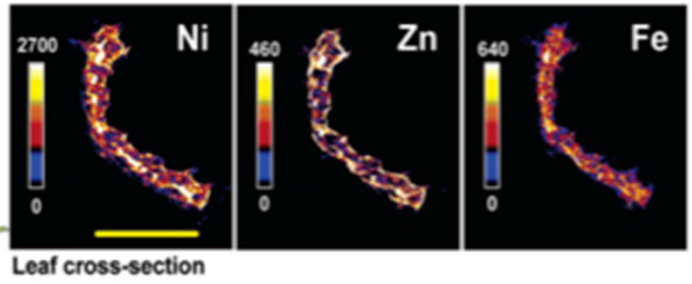

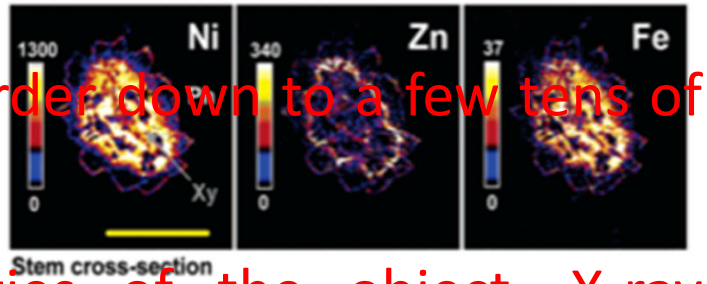

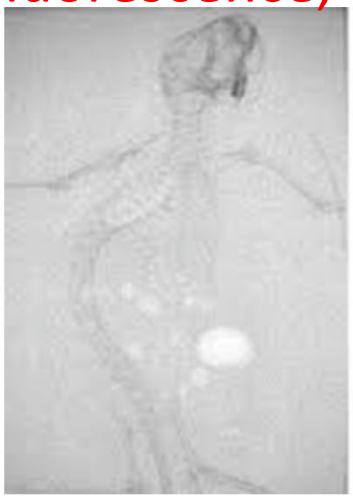

- Stunning imaging resolution at the order down to a few tens of nm
- Reveal interesting physical properties of the object, X-ray fluorescence, diffraction–enhanced imaging

Covered in lecture